Received: 2 October 2019 | Accepted: 30 March 2020
DOI: 10.1002/hyp.13767

RESEARCH ARTICLE

WILEY

Towards the representation of groundwater in the Joint UK Land Environment Simulator

Stamatis-Christos Batelis[1] | Mostaquimur Rahman[1] | Stefan Kollet[2,3] | Ross Woods[1] | Rafael Rosolem[1,4]

[1]Department of Civil Engineering, University of Bristol, Bristol, UK

[2]Institute of Bio- and Geosciences, Agrosphere (IBG-3), Forschungszentrum Jülich, Jülich, Germany

[3]Centre for High-Performance Scientific Computing in Terrestrial Systems, Geoverbund ABC/J, Jülich, Germany

[4]Cabot Institute, University of Bristol, Bristol, UK

Correspondence
Stamatis-Christos Batelis, Department of Civil Engineering, University of Bristol, Bristol, UK.
Email: s.batelis@bristol.ac.uk

Funding information
AMUSED, Grant/Award Number: NE/M003086/1; BEMUSED, Grant/Award Number: NE/R004897/1; WISE CDT, Grant/Award Number: EP/L016214/1; Cranfield University, Grant/Award Number: L0155; Natural Environment Research Council, Grant/Award Numbers: R004897, M003086; Engineering and Physical Sciences Research Council, Grant/Award Number: L016214

Abstract

Groundwater is an important component of the hydrological cycle with significant interactions with soil hydrological processes. Recent studies have demonstrated that incorporating groundwater hydrology in land surface models (LSMs) considerably improves the prediction of the partitioning of water components (e.g., runoff and evapotranspiration) at the land surface. However, the Joint UK Land Environment Simulator (JULES), an LSM developed in the United Kingdom, does not yet have an explicit representation of groundwater. We propose an implementation of a simplified groundwater flow boundary parameterization (JULES-GFB), which replaces the original free drainage assumption in the default model (JULES-FD). We tested the two approaches under a controlled environment for various soil types using two synthetic experiments: (1) single-column and (2) tilted-V catchment, using a three-dimensional (3-D) hydrological model (ParFlow) as a benchmark for JULES' performance. In addition, we applied our new JULES-GFB model to a regional domain in the UK, where groundwater is the key element for runoff generation. In the single-column infiltration experiment, JULES-GFB showed improved soil moisture dynamics in comparison with JULES-FD, for almost all soil types (except coarse soils) under a variety of initial water table depths. In the tilted-V catchment experiment, JULES-GFB successfully represented the dynamics and the magnitude of saturated and unsaturated storage against the benchmark. The lateral water flow produced by JULES-GFB was about 50% of what was produced by the benchmark, while JULES-FD completely ignores this process. In the regional domain application, the Kling-Gupta efficiency (KGE) for the total runoff simulation showed an average improvement from 0.25 for JULES-FD to 0.75 for JULES-GFB. The mean bias of actual evapotranspiration relative to the Global Land Evaporation Amsterdam Model (GLEAM) product was improved from −0.22 to −0.01 mm day^{-1}. Our new

JULES-GFB implementation provides an opportunity to better understand the interactions between the subsurface and land surface processes that are dominated by groundwater hydrology.

KEYWORDS
flow boundary, free drainage, groundwater, land surface model

1 | INTRODUCTION

It is widely known that groundwater (GW) is of paramount importance for water management, as it represents 97% of available freshwater resources worldwide (Guppy, Uyttendaele, Villholth, & Smakhtin, 2018). According to Alley, Healy, LaBaugh, and Reilly (2002), more than two billion people depend on groundwater supply as their main water source, while the vast majority of water for irrigation comes from groundwater sources (Siebert et al., 2010). Groundwater is also the last critical national resource during droughts (Famiglietti et al., 2011); thus, it will be key in future water management, knowing that climate change will likely increase the frequency of drought (e.g., Lehner, Döll, Alcamo, Henrichs, & Kaspar, 2006). By representing groundwater in large-scale models, we can understand and quantify the interactions between groundwater and climate, understand and quantify the two-way interactions between the subsurface with the surface and the atmosphere and support decision making in transboundary groundwater systems (Gleeson et al., 2019). Land surface models (LSMs) are now being applied for operational applications in global hydrology (e.g., Beck et al., 2017; Givati, Gochis, Rummler, & Kunstmann, 2016; Sutanudjaja et al., 2018). However, groundwater representation is still neglected in most LSMs; hence, it is crucial to incorporate such processes in order to improve the predictions of these models.

The soil domain of an LSM usually extends vertically from the surface to a depth of 2–5 m. With regard to conditions constraining water dynamics at the bottom of the soil domain, most LSMs still apply the free drainage condition (i.e., water flow at the bottom boundary of the model domain is controlled solely by gravity; JULES, CLM 4.0, HTESSEL, Noah, VIC, H08, CLASS) or a shallow aquifer ignoring the lateral flow (MATSIRO, ORCHIDEE). Only a few of them (CLM 4.5, Noah-MP) are fully coupled with a groundwater model below the soil domain.

Recently, improvements have been made towards to coupling groundwater models below LSMs and global hydrological models (e.g., de Graaf et al., 2017; de Graaf, Sutanudjaja, Van Beek, & Bierkens, 2015; Fan, Li, & Miguez-Macho, 2013; Fan & Miguez-Macho, 2011; Ganji & Sushama, 2018; Gedney & Cox, 2003; Gulden et al., 2007; Gutowski Jr et al., 2002; Guzman et al., 2015; Koirala, Kim, Hirabayashi, Kanae, & Oki, 2019; Maxwell et al., 2011; Maxwell & Miller, 2005; Niu, Yang, Dickinson, Gulden, & Su, 2007; Reinecke et al., 2019; Tian et al., 2020; Tian, Li, Wang, & Hu, 2012; Vergnes & Decharme, 2012; Yeh & Eltahir, 2005a, 2005b; York, Person, Gutowski, & Winter, 2002; Zeng et al., 2018). These studies generally showed that adding the groundwater component led to a more realistic partitioning of water components at the land surface.

There are two main classifications of groundwater coupling, namely, the empirical lumped GW models and the physically based distributed GW models (Tian et al., 2012). Regarding their dimension, this can be either a one-dimensional (1-D) model (e.g., Gedney & Cox, 2003; Maxwell & Miller, 2005; Yeh and Eltahir, 2005a; Niu et al., 2007; Huang et al., 2019), two-dimensional (2-D) model (e.g., Fan & Miguez-Macho, 2011; Vergnes & Decharme, 2012) or 3-D model (e.g., Gutowski Jr et al., 2002; Maxwell et al., 2011; Tian et al., 2012; York et al., 2002). In the 1-D coupling, the soil domain is extrapolated for a few tens of meters. The downward flux of the free drainage assumption is replaced by a two-way flux. However, lateral flux is not represented in this type of coupling. In the 2-D coupling, the total head of the aquifer or the recharge is calculated based on the neighbouring cells. In that case, the lateral flow is included in the calculation of the flux that interacts between the aquifer and the soil domain of the LSM. Finally, in the 3-D coupling, the lateral flow and the vertical flux are calculated based on the neighbouring cells throughout the soil column, from the soil to the aquifer for both saturated and unsaturated zones. The baseflow usually is extracted from the aquifer, as a percentage of the water table depth using exponential equations. Considering that the horizontal transport of groundwater is important on smaller spatial scales, this makes the use of a 3-D model suitable for regional studies and the use of 1-D model suitable for global studies (Bierkens et al., 2015; Niu et al., 2007). Some schemes were implemented in uncoupled mode, as recharge from LSM was the input to GW models (e.g., de Graaf et al., 2015, 2017; Fan & Miguez-Macho, 2011).

The Joint UK Land Environment Simulator (JULES) is a widely used land surface model, developed by the UK MetOffice, and used for operational services and research to simulate the energy, carbon and water balance between the land surface and the lower atmosphere (Best et al., 2011; Clark et al., 2011). The hydrological components of JULES have been tested for runoff predictions at monthly and inter-annual scales (Gudmundsson et al., 2012a & 2012b; MacKellar, Dadson, New, & Wolski, 2013) and at daily resolution (Dadson & Bell, 2010; Dadson, Bell, & Jones, 2011; Martínez-de la Torre, Blyth, & Weedon, 2019; Weedon et al., 2015; Zulkafli, Buytaert, Onof, Lavado, & Guyot, 2013). In a model intercomparison experiment for simulating the inter-annual variability of observed runoff in Europe (Gudmundsson, Tallaksen, et al., 2012), JULES was ranked third out of 10 large-scale hydrological models. Dadson and Bell (2010) compared the two-river flow routing schemes of JULES

for 10 large catchments. The model performance was poor and only for one catchment the Nash Sutcliffe efficiency for the optimized simulations was higher than 0.5. Weedon et al. (2015) applied nine distributed hydrological models, including JULES, to simulate the daily runoff at the Thames catchment. The evaluation was based on the cross-spectral analysis and they found that JULES' performance depended on the configuration that was used (i.e., JULES-TOPMODEL, JULES-PDM, JULES) with JULES-TOPMODEL producing a slightly better performance.

The current JULES model relies on the more typical free drainage assumption. Le Vine, Butler, McIntyre, and Jackson (2016) made the first attempt to couple a groundwater model with JULES in a chalk groundwater dominated catchment. In particular, they coupled the ZOOMQ3D groundwater model (Jackson, 2001) with JULES to simulate the Kennet catchment, a tributary of the Thames River. They extended the soil depth from 3 to 6 m and they used the recharge from JULES as the upper boundary condition to the groundwater model offline. After an extensive calibration, they managed to improve the water balance, the soil moisture and the runoff simulation. However, with this type of coupling, their model cannot simulate the water table depth and the feedback between saturated and unsaturated zones.

The free drainage scheme has some limitations as it does not allow for a two-way interaction between the unsaturated zone and the water table (Maxwell & Miller, 2005). Rahman, Rosolem, Kollet, and Wagener (2019) showed that the free drainage assumption exacerbates drying because there is no physical constraint at the bottom of the soil column to prevent the water to be retained within the soil domain. As a consequence, excessive drying of soils will lead to reduced rates of evapotranspiration and alter the contribution of baseflow to river discharge and the water partition in general (e.g., Kollet & Maxwell, 2008). Rahman et al. (2019) provided a new theoretical development of a simplified groundwater model for use in Earth system model applications. This model allows for two-way interactions between saturated and unsaturated zones.

The aim of this article is to understand the impact of adding a new hydrological component related to groundwater processes into the JULES model while evaluating its performance.

Our study focuses on addressing two main research questions:

1 Under which conditions (e.g., water table depth, soil type) can we identify improvements in the JULES model when groundwater dynamics are explicitly represented?
2 How do soil water dynamics, due to explicit representation of groundwater, potentially impact other hydrological fluxes at the land surface (e.g., streamflow and evapotranspiration) at the regional scale?

Here, we implement a fully coupled groundwater parameterization within JULES and assess the potential impact on key hydrological variables in the model. This groundwater parameterization is based on the theoretical development presented by Rahman et al. (2019), which has not yet been tested with an LSM. This model assumes pressure and flux continuity at the interface between the lowest soil layer and the underlying aquifer. Thus, we can calculate the position of the water table based on the pressure head obtained with the soil moisture estimate in the last soil layer of the soil domain. Our approach is different from the approach of Le Vine et al. (2016), since we apply a dynamic groundwater model that interacts with JULES in real time and allows for two-way interaction between aquifer and soil domain. We will use a more complex 3-D hydrological model as a benchmark in a set of synthetic experiments. We will then apply our model in a regional domain characterized by groundwater-dominated catchments in the UK. The model's ability to represent soil moisture patterns, streamflow and evapotranspiration within the domain are compared against physical characteristics of the regional domain as well as observations from UK streamflow database and evapotranspiration products from remote sensing.

2 | DATA AND METHODS

2.1 | Joint UK Land Environment Simulator (JULES)

The JULES model (Best et al., 2011; Clark et al., 2011) requires eight meteorological forcing variables, namely, wind speed, air temperature, surface downwelling longwave and shortwave radiation, specific humidity, atmospheric pressure and rainfall and snowfall rates. Ancillary data include land cover and soil types. Land cover data are used to link regional characteristics to vegetation parameters (Clark et al., 2011, tables 1, 2), and the soil type map is used to prescribe soil hydrology parameters, as described in Best et al. (2011, table 3).

Here, we briefly introduce the key components of the soil hydrology in JULES model, which are relevant for our study. For further information about JULES, please refer to Best et al. (2011) and Clark et al. (2011).

The default JULES model has four soil layers defined with different thickness, namely, 0.10, 0.25, 0.65 and 2 m. In this study, we have modified the vertical discretization to be more consistent with the groundwater model and the additional simulations used for testing (i.e., benchmark model and additional hydrological models—see Subsections 2.3.1 and 2.3.2). In this case, all JULES model versions discussed in this study have been set up with evenly spaced 20 cm thick soil layers from surface to 3 m depth for the infiltration experiment and the regional analysis and 10 cm layers for the tilted-V experiment. We refer to this version of the model as JULES-FD (free drainage).

At each node n, the soil water content θ_n is updated using the 1-D finite difference form of the Richards equation to estimate the transport of moisture. Richards' equation is the combination of continuity (1) and Darcy's law (2) that models the vertical fluxes.

$$\frac{d\theta_n}{dt} = W'_{n-1} - W'_n - E'_n, \tag{1}$$

$$W' = K_h\left(\partial\Psi/\partial z_n + 1\right). \tag{2}$$

where W'_{n-1} and W'_n are the diffusive fluxes flowing in from the upper layer and to the layer below, respectively. E'_n is the evapotranspiration extracted by plant roots in the layer, K_h is the hydraulic conductivity (mm/s), Ψ is the soil water suction (m) and z is the soil depth (m). In Equation (1), the top boundary condition is the infiltration of water at the surface and the bottom boundary condition is the free drainage (Figure 1a), which contributes to the subsurface runoff (Best et al., 2011). The water table and the lateral flow in the saturated zone are not explicitly represented in JULES-FD.

The soil hydraulic parameters are calculated from soil texture information, using the Van Genuchten (1980) hydraulic relationships.

$$S_\theta = \frac{\theta - \theta_r}{\theta_s - \theta_r} = \frac{1}{\left[1 + (\alpha_\nu \Psi)^n\right]^m}, \quad (3)$$

where θ is the soil moisture ($m^3\ m^{-3}$), θ_r is the residual soil moisture ($m^3\ m^{-3}$), θ_s is the soil moisture at saturation ($m^3\ m^{-3}$), S_θ is the effective saturation and α_ν, n and m are parameters computed based on soil parameters with the following relationship $m = a - 1/n$. The hydraulic conductivity (K_h) is calculated from the following equation (Schaap, Leij, & Van Genuchten, 2001).

$$K_h = K_{hs} S_\theta^\xi \left[1 - \left(1 - S_\theta^{1/m}\right)^m\right]^2, \quad (4)$$

where K_{hs} is the hydraulic conductivity for saturated soil and ξ is a coefficient fixed at 0.5.

In relation to surface runoff generation, there are two mechanisms to produce surface runoff, namely, the infiltration excess and saturation excess mechanisms in JULES. The infiltration excess runoff is calculated considering both the throughfall and the grid-box mean infiltration (Best et al., 2011) based on the equations by Johannes Dolman and Gregory (1992). Infiltration excess occurs when the rainfall rate is higher than the hydraulic conductivity of the topsoil. In order to account for subgrid heterogeneity of soil moisture and saturation excess runoff, JULES uses the probability distribution model (PDM; Moore, 2007). This method describes heterogeneity in the topsoil layer (1 m). The PDM scheme requires the prescription of two parameters, namely, the depth of the topsoil (dz_{pdm}) and an exponent coefficient for the Pareto distribution of soil water holding capacity (b_{pdm}). The default values for dz_{pdm} and b_{pdm} are 1 m and 1, respectively. According to the theory, higher values of b_{pdm} increase the runoff because for a given soil moisture storage, a higher b_{pdm} leads to higher saturated fraction (fig. 6a of Moore, 1985), which leads to higher surface runoff (Clark & Gedney, 2008). It is found that b_{pdm} is more sensitive than the dz_{pdm} in our preliminary analysis and in other studies (Bakopoulou, 2015), whereas dz_{pdm} is usually ignored (Martínez-de la Torre, 2019) or constrained by data (Dadson et al., 2011; MacKellar et al., 2013).

Finally, the river routing scheme in JULES is based on the rapid flow model (RFM; Bell, Kay, Jones, & Moore, 2007), which estimates the approximation of the 1-D kinematic wave equation with lateral inflow. The RFM uses six globally constant parameters, namely, two surface and two subsurface wave celerities for river or land cells and two return flow fractions.

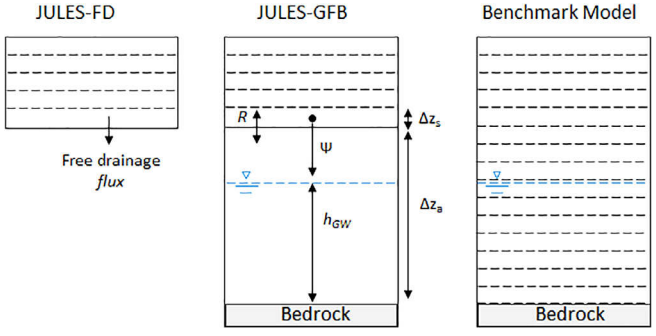

FIGURE 1 (a) Schematic overview of JULES-FD with the free drainage assumption, (b) JULES-GFB with the simplified groundwater representation and (c) the full 3-D hydrological model used as a benchmark (shown here as a 1-D column for simplicity)

2.2 | Groundwater flow boundary parameterization

In this study, we adapt the concept of a free-surface groundwater flow boundary (GFB) condition, described by Rahman et al. (2019), which is targeted to large-scale hydrological modelling. The GFB concept was substantiated using synthetic experiments in Rahman et al. (2019).

The fundamental equation that governs the estimation of the groundwater flow in two horizontal dimensions can be written as (Meenal & Eldho, 2011; Pinder & Bredehoeft, 1968; Prickett & Lonnquist, 1971):

$$\frac{S\partial H}{\partial t} = \nabla(T\nabla H) + R, \quad (5)$$

where H is the total head (L), T is transmissivity ($L^2\ T^{-1}$), R is the recharge flux ($L\ T^{-1}$) and S is the specific yield (–). The coupling between the GFB groundwater model and JULES is based on recharge from the groundwater model. This is the flux that links the two models and interacts with them (flux R in Figure 1b).

The GFB approach described above considers two major assumptions (Rahman et al., 2019). The first assumption is the pressure and flux continuity at the interface between the lowest soil layer and the underlying aquifer. Following from this assumption, the saturated depth (h_{GW}) is calculated in JULES-GFB using the pressure head at the lowest soil layer as follows:

$$h_{GW} = \Delta z_a + {}^{\Delta z_s}/_2 - \Psi, \quad (6)$$

where Δz_a is aquifer thickness (L), Δz_s is the thickness of the last soil layer (L) and Ψ is the pressure head (L) at the last soil layer (Figure 1b). Then, adding to h_{GW} the datum from the bedrock, we can get the total head (H).

The second assumption is that the change in the saturated depth (Δh_{GW}) is negligible compared with the absolute value of h_{GW} (i.e., $\Delta h_{GW} << h_{GW}$). This assumption allows the calculation of T at each model time step as follows:

$$T = K_{hs} h_{GW}. \quad (7)$$

Equations (5)–(7) show the formulation of the GFB described in Rahman et al. (2019), which serves as the basis for the representation of groundwater dynamics in JULES-GFB. However, a few additional steps are necessary to incorporate the GFB concept into JULES.

First, we follow similar assumptions made by Niu et al. (2007) for special cases when the water table is so high that it is located within JULES' soil domain. In this case, we assume there is no vertical exchange of water between the aquifer and the soil domain. As a result, the recharge flux in the saturated portion of JULES soil domain is based only on the lateral flow (Equation 8), while the remaining unsaturated soil layers are updated as usual, following Equation (5).

$$-\nabla(T\nabla H) = R. \quad (8)$$

Second, a pseudo layer is introduced (acting as a 'coupler' layer) between the soil domain and the aquifer, in order to calculate the derivative of flux with soil water content ($\frac{dW_k}{d\theta_k}$) that is needed for calculating the soil moisture increment every timestep. JULES does not calculate this derivative at the lowermost soil layer. Thus, a pseudo layer is needed to calculate the derivative in the last true layer of the soil domain, above the pseudo layer.

Our calculation of groundwater table depth is dependent entirely on the pressure head at the last layer of the JULES soil domain. Because of the way of our calculation, any abrupt change in the pressure head between two consecutive timesteps at the last layer of JULES could create oscillations in the groundwater table depth. Note that abrupt changes in the pressure head in the last layer are likely, especially due to the direct Gaussian solver of JULES. In order to reduce those numerical oscillations, a noniterative Picard method (Paniconi, Aldama, & Wood, 1991; Tan, Phoon, & Chong, 2004) is introduced between timesteps (Equation 9).

$$R^{t+1,l+1} = \frac{R^{t+1,l} + R^t}{2}, \quad (9)$$

where t is the timestep and l is the number of iterations. One iteration is sufficient to remove the oscillations and to apply the new model explicitly. Note that if the pressure head is such that the water table falls below the bedrock for a given timestep, then the model reverts back to the free drainage parameterization.

In summary, the potential advantages of this new scheme are the replacement of the often unrealistic free drainage assumption from JULES-FD; the lateral saturated flow interaction, as the calculation of the water table is based on the neighbouring cells and the impacts on soil moisture content at the topsoil and the surface, where the water table intersects the surface and generates streams.

2.3 | Experimental design

In this study, we reproduce the same synthetic cases used in Rahman et al. (2019) and in Kollet et al. (2017) in order to compare the new JULES-GFB model with a widely used hydrological model (ParFlow), used as benchmark in that work. ParFlow is a 3-D variably saturated subsurface flow model that can simulate the water cycle between the bedrock and the top of the plant canopy. Further information about ParFlow can be found in Ashby and Falgout (1996), Kollet and Maxwell (2006) and Maxwell (2013). In addition, we also evaluate JULES-GFB at the regional scale using observations and remotely sensed products for actual evapotranspiration from the Global Land Evaporation Amsterdam Model (GLEAM) dataset.

2.3.1 | Synthetic infiltration experiment

We use a column experiment to test and compare the infiltration mechanisms in each model without the impact of lateral flow (Figure 2a). We evaluate how the wetting front changes after an applied rainfall pulse interacts with the aquifer (in both JULES-GFB and the benchmark ParFlow model), in comparison with JULES-FD. Each experiment comprises a 5-day simulation with an applied constant rainfall rate of 5 mm hr^{-1} in the first 10 hr of the experiment, assuming no surface water loss through evaporation. The temporal resolution is set to 15 min. The setup is the same used by Rahman et al. (2019).

In order to evaluate model performance, we use the mean bias of soil wetness fraction (unitless), which is defined as the fraction corresponding to the ratio of actual moisture content to maximum soil moisture possible for each soil layer (ranging from 0 to 1, which corresponds to fully dry and fully wet, respectively). The bias is calculated from the soil profiles (i.e., surface to 3 m depth) for each of the two JULES versions (JULES-FD and JULES-GFB) relative to the results from the ParFlow benchmark model obtained from Rahman et al. (2019). By assessing mean bias, the results will indicate conditions where models underestimate (overestimate) the benchmark model as a result of drier (wetter) soil wetness conditions. Our comparisons use a combination of 12 different soil types (parameters defined according to Table Data S1 in Appendix) and 12 different initial conditions of water table depth (from shallow, located at 0.25 m, to deeper, located to maximum depth of 30 m below the surface, following Rahman et al., 2019).

2.3.2 | Synthetic groundwater discharge experiment

For this experiment, we introduce the effects of topographic slope in driving the subsurface flow in a tilted-V shaped synthetic catchment (Figure 2b). Our specific objective here is to evaluate the contribution of the lateral flow to the simulated discharge at the outlet. We follow the same setup used in the integrated hydrologic model

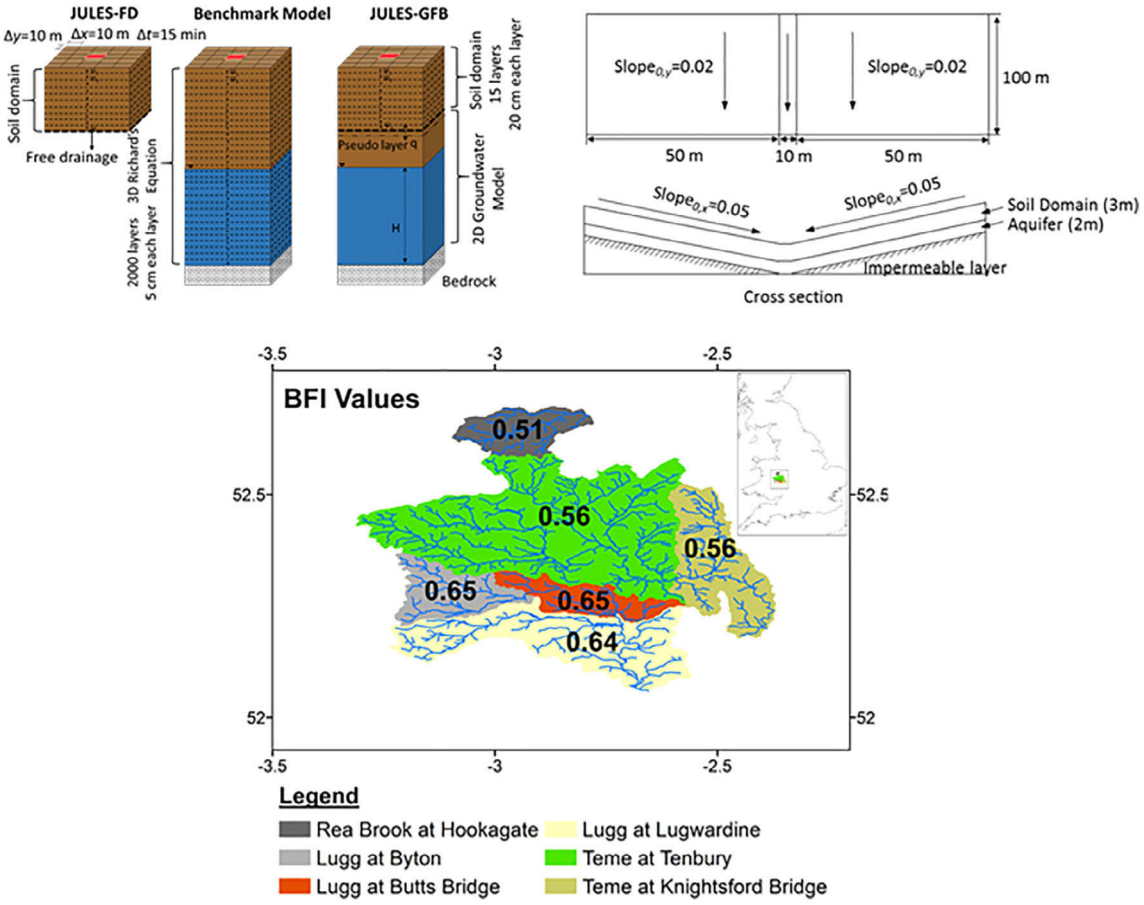

FIGURE 2 Schematic overview of experiments in the study: (a) infiltration single-column synthetic experiment, (b) synthetic groundwater discharge experiment and (c) UK regional domain

intercomparison project 2 (IH-MIP2; Kollet et al., 2017), which also includes the benchmark ParFlow model. In addition, the IH-MIP2 includes the simulation results from additional integrated hydrological models, which allows us to more robustly evaluate the overall performance of JULES-GFB with respect to a range of similar models. In addition to ParFlow, IH-MIP2 models include the advanced terrestrial simulator (ATS) (Coon, Moulton, & Painter, 2016; Painter et al., 2016), Cast3M (Weill, Mouche, & Patin, 2009), CATchent hydrology (CATHY) (Bixio et al., 2002; Camporese, Paniconi, Putti, & Orlandini, 2010), GEOtop (Endrizzi, Gruber, Dall'Amico, & Rigon, 2014; Rigon, Bertoldi, & Over, 2006), HydroGeoSphere (HGS) (Aquanty, 2015) and MIKE-SHE (Abbott, Bathurst, Cunge, O'connell, & Rasmussen, 1986; Butts, Payne, Kristensen, & Madsen, 2004). For details about the IH-MIP2 and its models, please refer to Kollet et al. (2017).

The tilted V-shaped topography is perfectly symmetrical in both directions with spatial resolution defined as 10 m. The width of the V-shaped catchment is 110 m, corresponding to two 50 m slopes separated by a 10 m wide river channel. The length of the catchment is 100 m (Figure 2b) and the soil column is 5 m deep at all locations. The slope in the x direction is $Slope_{0,x}$ = 0.05 and in the y direction is $Slope_{0,y}$ = 0.02. The water table depth is initialized at 2 m below land surface with hydrostatic conditions vertically. We simulate 120 hr with no rainfall and no loss from evapotranspiration and run with timestep of 5 seconds. We specify the soil properties based on a sandy soil following Kollet et al. (2017). Our JULES-GFB and JULES-FD simulations are run without the river flow model parameterization due to the small size of the catchment. We, therefore, assume that the surface storage from all the cells within the domain contribute to the outlet of the catchment in the same timestep. The evaluation of JULES-GFB and JULES-FD will be based on bias and linear correlation computed against the benchmark and other models used in IH-MIP2 for saturated and unsaturated storages, as well as for the outlet discharge. In JULES-FD, we extended the soil domain from 3 to 5 m to directly compare the same initial conditions in terms of saturated and unsaturated storages to other IH-MIP2 models.

2.3.3 | Regional experiment

Synthetic experiments can be useful tools to validate new model developments. However, they pose the limitation of using ideal conditions and forcing, often assuming homogeneous spatial characteristics (soil type, land use). Here, to test the model further, we compare our

new JULES-GFB model against the JULES-FD in a real-world application. In this case, the experiment is carried out over a regional domain in the UK, which consists of six neighbouring catchments (with individual areas greater than 100 km^2 and near natural conditions) characterized by being groundwater dominated (i.e., relatively high Base Flow Index, BFI; Figure 2c and Table 1). The elevation map is derived from Hydrological data and maps based on Shuttle Elevation Derivatives at multiple Scales (HydroSHEDS; Lehner, Verdin, & Jarvis, 2008) with 1 km spatial resolution. The elevation ranges from 0 to 980 m within the domain (Figure 3a). The elevation map is postprocessed in order to provide flow directions following the methodology presented in Maxwell et al. (2009).

The Land Cover Map 2007 (LCM2007) (Morton et al., 2011) is used to obtain spatially distributed land cover type information. In addition, soil albedo values are derived from the land use map based on Houldcroft et al. (2009). Dominant vegetation types within the domain are shrubs (50%) and C3 grasses (43%), as shown in Figure 3b.

Soil parameters are derived for the regional domain from the land information system provided by the Cranfield University. This dataset is based on field work and covers both England and Wales (Hallett, Sakrabani, Keay, & Hannam, 2017). Soil classes are shown in Figure 3c with dominant clay loam (31%) and silty clay loam (30%) classes within the domain. Note that we did not apply any parameter calibration to JULES-GFB. Instead, we used an ad hoc sensitivity analysis of the aquifer conductivity to identify the impact on the model performance.

In order to simplify our initial test with JULES-GFB, we define key aquifer properties with spatially uniform information from domain-average parameters also obtained from the land information system. Furthermore, we assume a homogeneous depth of aquifer equal to 100 m, which is a common approach for large-scale groundwater applications (e.g., Condon & Maxwell, 2015; Keune et al., 2016). We set a constant specific yield to 0.2, following a similar approach by previous studies (Ganji & Sushama, 2018; Niu et al., 2007). The focus of this study is to initially test the introduction of the groundwater parameterization into the JULES model and setting homogeneous properties is sometimes a common strategy (e.g., Condon & Maxwell, 2015; Niu et al., 2007). The impact of introducing heterogeneous aquifer properties and depth to bedrock is beyond the scope of this study and can be further tested in the future.

The vertical discretization of JULES-FD and JULES-GFB is 0.2 m, similar to the column-scale experiment with both model versions extending their soil domain depth to 3 m. We used a timestep of 10 min, which ensures satisfactory runoff predictions without adding too much computational time.

The regional forcing data are obtained from the climate, hydrology and ecology research support system (CHESS) dataset (Robinson, Blyth, Clark, Finch, & Rudd, 2016). CHESS data are available at daily temporal resolution and 1 km spatial resolution covering the entire Great Britain. The forcing data are downscaled from daily to 10-min timestep using the downscaling tool of JULES and the daily temperature range, which is obtained from CHESS database. The regional simulation encompasses the year between 2008 and 2012. The different JULES versions are each individually spun-up following common procedures. Particularly to our case, we cycle the 2008–2012 period repeatedly until the mean monthly soil moisture does not deviate by more than 0.1% from the previous year, following the same protocol used for the large-scale biosphere-atmosphere experiment in Amazônia, model intercomparison project (LBA-MIP) (de Goncalves et al., 2008). The initial soil moisture initialize for the first cycle is set so that all soils layers across the domain have a soil wetness fraction of 0.95. The 5-year period selected shows temperature ranges from −8 to about 22°C with strong seasonality and average annual precipitation of 871 mm (Figure 4). The meteorological conditions during selected 2008–2012 period show a mean annual temperature of 9.4°C and mean annual precipitation of 871 mm, which are very similar to the 1981–2015 climatological record for the region calculated from the CHESS (9.3°C and 886 mm, respectively).

As described in Section 2.1, PDM is the subgrid variability model based on statistical parameterization to simulate saturation excess runoff. For JULES-FD, we tested different values of b_{pdm}, ranging from 0.2 to 1. In JULES-GFB, PDM is not used because JULES-GFB can directly simulate saturation excess in those cells, which have the water table at the surface.

In this experiment, we evaluate all versions of JULES against daily streamflow data from individual catchments (Figure 2 and Table 1) provided by the National River Flow Archive (NRFA), covering 2008–2012 period. We choose mean bias, the Pearson correlation

TABLE 1 Catchment characteristics for the regional analysis

Name	Catchment area (km^2)	Mean flow (m^3 s^{-1})	BFI	Rainfall (mm year^{-1})
Lugg at Byton	203	3.9	0.65	1,039.1
Lugg at Butts Bridge	371	6.0	0.65	981.7
Lugg at Lugwardine	886	10.8	0.64	845.4
Teme at Tenbury	1,134	14.6	0.56	755.1
Teme at Knightsford Bridge	1,480	18.2	0.56	736.4
Rea Brook at Hookagate	178	1.7	0.51	822.9

Abbreviation: BFI, Base Flow Index.

[a]BFI was computed by NRFA based on the archived record of gauged daily mean runoff.

[b]Mean flow and Annual Mean Rainfall are based on NRFA and CHESS datasets from 1970 to 2015, respectively.

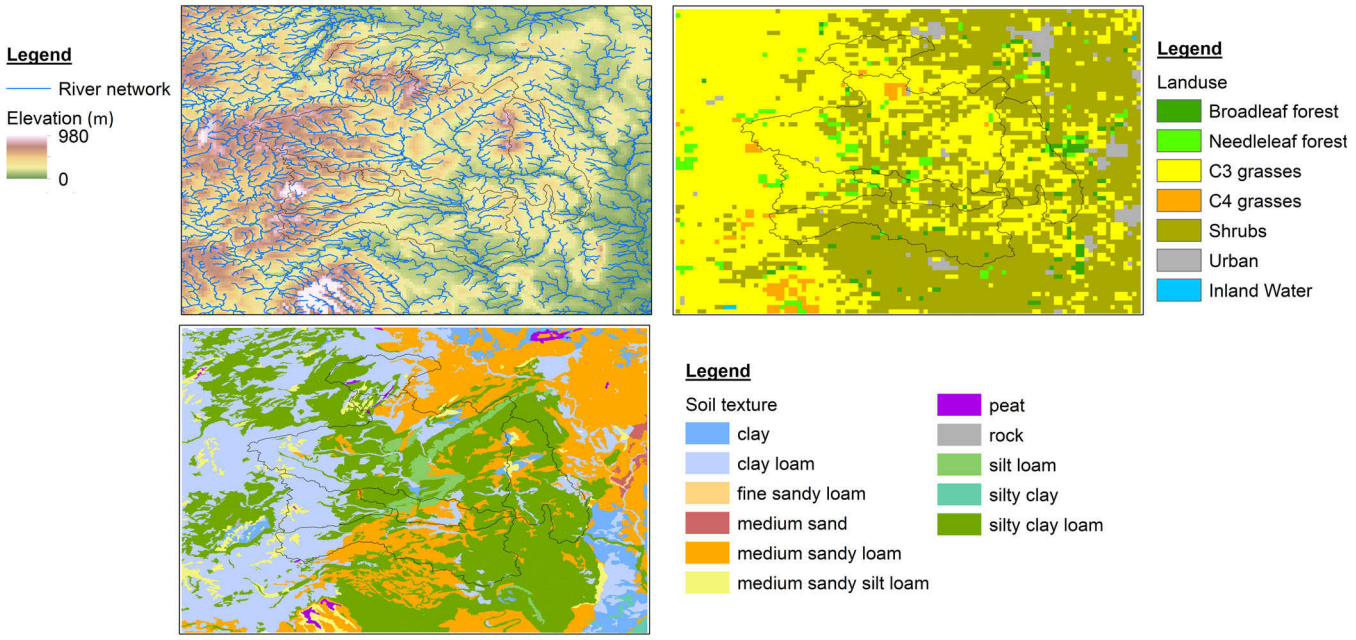

FIGURE 3 Physical characteristics of the regional domain experiment: (a) river network and topography (HydroSHEDS); (b) land cover (Land Cover Map 2007) and (c) soil texture (Land Information System)

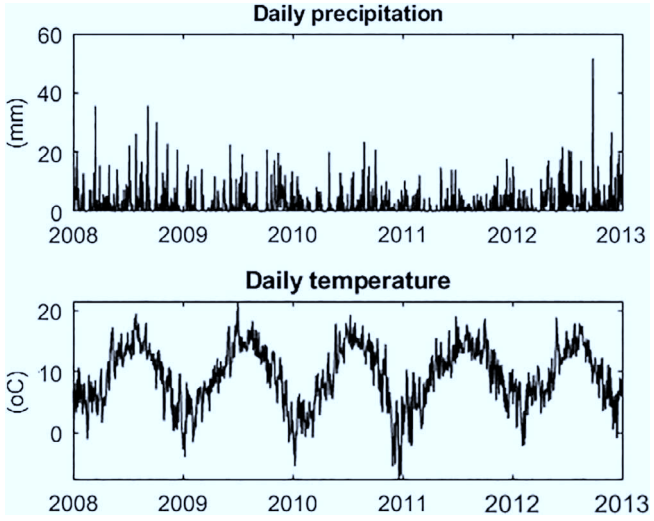

FIGURE 4 Daily time-series of domain average input meteorological forcing for precipitation (m) and air temperature (°C) used in the regional experiment

coefficient and the Kling-Gupta Efficiency (KGE) (Gupta, Kling, Yilmaz, & Martinez, 2009), as model performance metrics.

In addition, we test these versions of JULES in representing the evapotranspiration flux within the domain and we compare model estimates against the daily Global Land Evaporation Amsterdam Model (GLEAM) (Martens, Waegeman, Dorigo, Verhoest, & Miralles, 2018; Miralles et al., 2011) dataset (version 3.3a). This dataset calculates evapotranspiration from the water balance equation based on satellite data to estimate the different components of the water cycle. The dataset is freely available and widely used (e.g., Forzieri, Alkama, Miralles, & Cescatti, 2017; Martens et al., 2018).

3 | RESULTS

3.1 | Synthetic infiltration experiment

Figure 5 depicts the soil moisture profile from the land surface to 3 m depth for JULES-FD (on the left), the ParFlow benchmark model (middle) and JULES-GFB (right) for three different combinations of soil type and initial water table depth (WTDi). The simulation is carried out for 5 days with a constant rainfall rate of 5 mm hr^{-1} during the first 10 hr only and with no water loss through evaporation.

We observe two distinct behaviours from the simulations. First, for the two cases where the water table is initialized within the soil domain of JULES (i.e., shallower than 3 m), JULES-FD is unable to retain the soil moisture, resulting in much drier soil moisture profiles when compared with the benchmark model. This behaviour is even more pronounced for relatively coarser textured soil types (e.g., sand), despite the initial water table being very close to the surface (i.e., at 0.5 m depth). The quick drying behaviour observed at the beginning is a result of initially high hydraulic conductivity as a result of wet initial conditions. This drying behaviour is sustained until the end of the simulation in JULES-FD due to a lack of physical constrain at the bottom of the domain (i.e., gravity flow drives loss of water leaving the bottom of the soil domain). Unlike the JULES-FD results, the new JULES-GFB shows remarkably good agreement with the benchmark model in both shallow water table cases shown in Figure 5, except for some minor differences close to the surface that

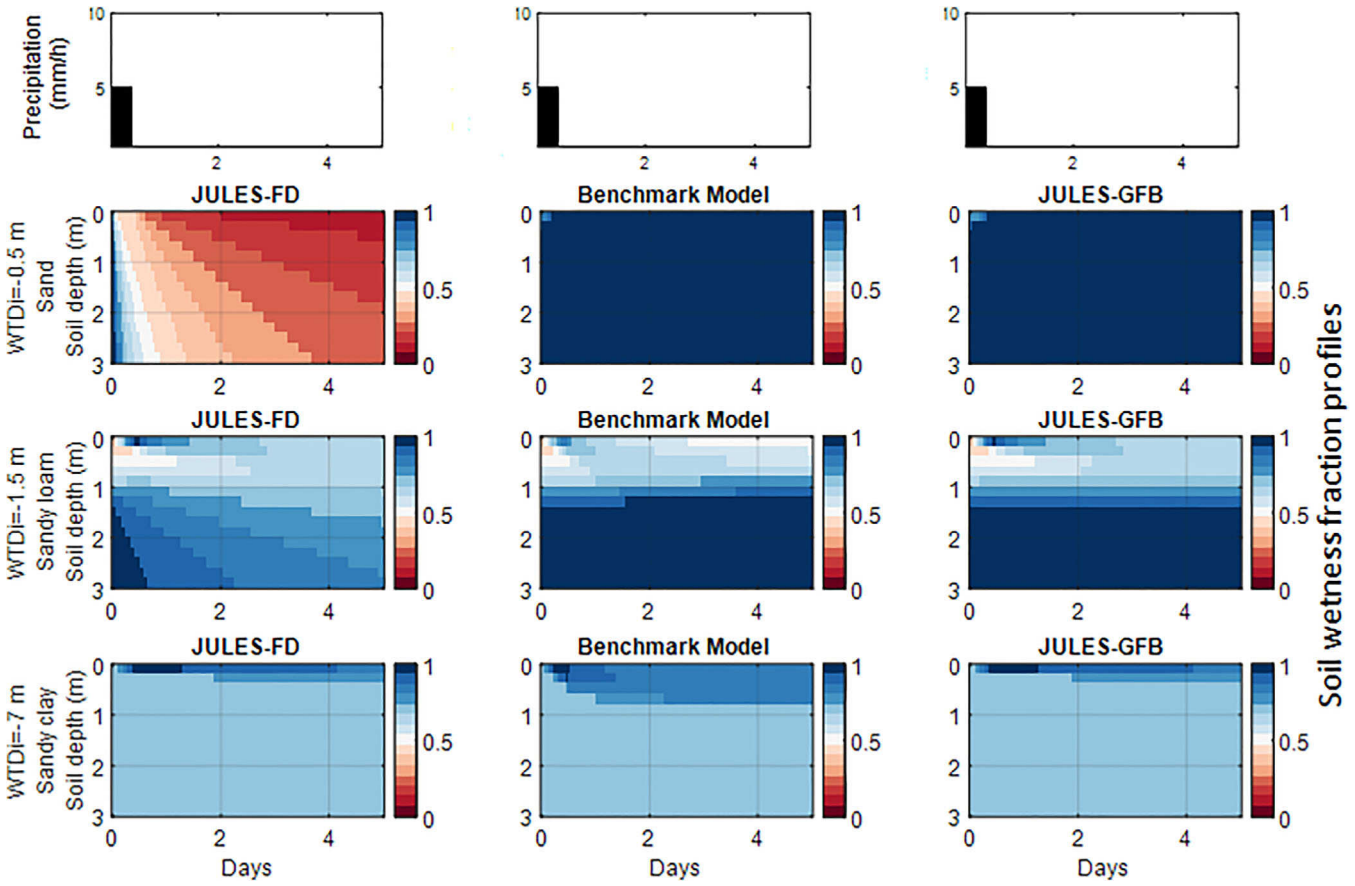

FIGURE 5 Examples of soil wetness fraction profiles within the JULES soil domain comparing the JULES-FD (left) and the new JULES-GFB approach (right) against the benchmark model simulations (centre), for the infiltration experiment

are related to the different water partitioning in ParFlow, compared with the two JULES models.

Second, we notice that when the water table is initialized outside of the soil domain in the model (i.e., deeper than 3 m), there are only minor differences between JULES-FD and JULES-GFB in the soil moisture dynamics within the profile. In addition, we observe some differences for both JULES versions from the benchmark model. This suggests that improvements from using JULES-GFB instead of JULES-FD are expected to occur more often for cases where the water table is shallow and for relatively coarse soil types.

In order to investigate this result more widely, we carried out a number of simulations using different combinations of soil types and initial water table depths. We test typical 12 different soil types with 12 different initial water table depths, resulting in a total of 144 combinations. For each combination, we calculate the mean bias between each of the JULES versions (i.e., FD or GFB) against the benchmark model for the entire 5-day simulation period (Figure 6). In this case, we use the soil moisture profile corresponding to the domain defined between the surface and down to 3 m depth (like those shown in Figure 5). The results in Figure 6 corroborate the selected example cases shown in Figure 5. JULES-FD errors suggest systematically drier conditions within the top 3 m of the domain with slightly worse performance for relatively coarse soils. Conversely, the new JULES-GFB model is characterized by very low mean bias across different combinations, when the water table is initialized within the 3 m soil depth. However, the deviation from the benchmark model, when the water table is initialized below 3 m depth, reveals no differences between JULES-FD and JULES-GFB. As expected, most of the impact of having the new JULES-GFB model is observed for shallow water table cases.

3.2 | Synthetic groundwater discharge experiment

Figure 7 compares JULES-GFB with the IH-MIP2 models in terms of storage dynamics of the saturated and unsaturated zones (averaged over the entire model domain), as well as outlet discharge rates. The behaviour of JULES-GFB (red line) is widely consistent with the other IH-MIP2 models (grey lines) and the benchmark model in terms of dynamics (linear correlation) and overall magnitude (mean bias), with both computed relative to the benchmark model (Table 2). On the contrary, JULES-FD shows a very distinct behaviour from all the other models due to the different assumption of the free drainage parameterization.

The initial reduction in saturated storage of JULES-GFB is consistent with water moving downwards and slowly contributing to the outlet streamflow (Figure 7a). All models are able to capture this initial

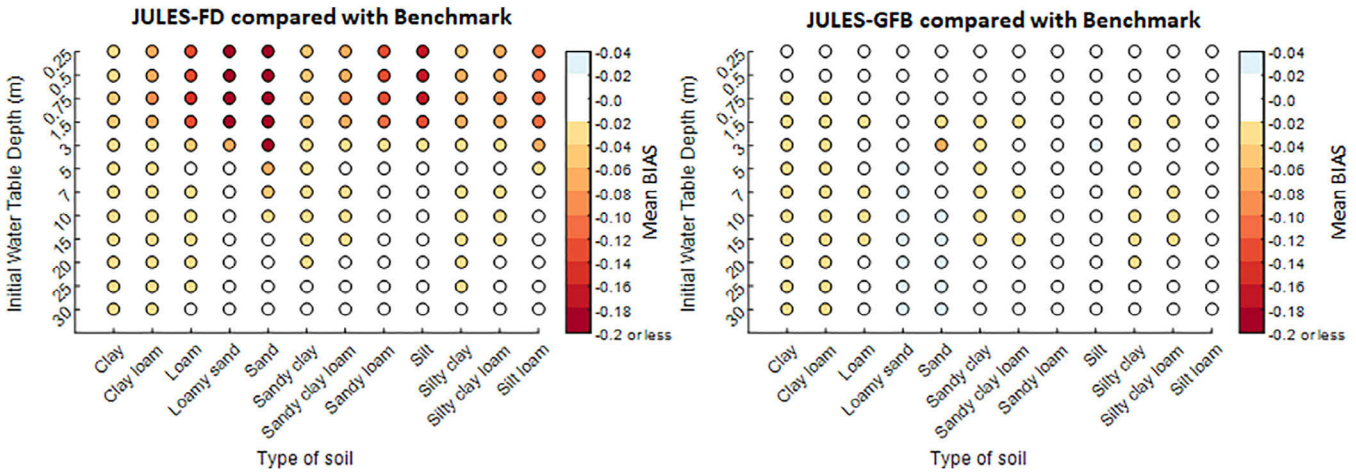

FIGURE 6 Overall model performance for the infiltration experiment computed within the soil domain as mean bias (bias) with respect to the benchmark model: (left) JULES-FD and (right) JULES-GFB model

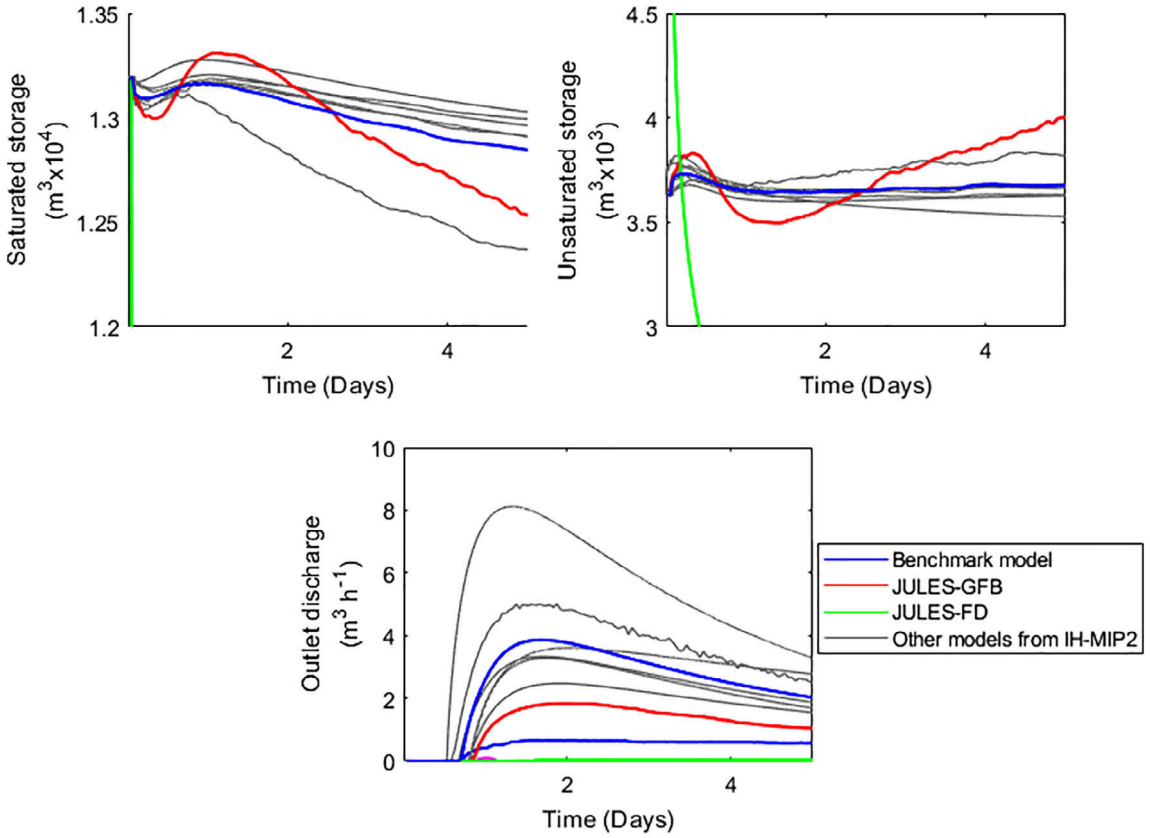

FIGURE 7 Comparison of (a) saturated storage, (b) unsaturated storage and (c) outlet discharge: JULES-GFB shown as red line, JULES-FD as green line and benchmark model as blue line. The grey lines correspond to other six integrated surface-subsurface hydrological models (IHSSMs) investigated in the IH-MIP2 study (see Kollet et al., 2017)

behaviour with some expected model-to-model differences. Interestingly, the JULES-GFB model shows the highest amplitude in change of saturated storage initially, when compared with other models, although the overall magnitude appears to be consistent with the average behaviour of all models. The reason for this steep behaviour may be because in JULES-GFB, the water from the soil domain instantly reaches the water table. As discussed by Rahman et al. (2019), this behaviour will tend to happen even faster for relatively coarse soils given the intrinsic limitations of linearly extrapolating pressure head values from bottom of soil domain to where the water table is located. Towards the end of the first day, we observe in all IH-MIP2 models a consistent small increase in the saturated storage followed

TABLE 2 Performance metrics for the tilted-V synthetic experiment computed against benchmark model (ParFlow)

	JULES-FD	JULES-GFB	Models in IH-MIP2
Saturated storage			
Bias (m^3)	−12,911	−53	−280 to 145
Correlation	0.157	0.965	0.965 to 0.996
Unsaturated storage			
Bias (m^3)	−1,542	64	−67 to 83
Correlation	0.34	0.56	0.15 to 0.94
Runoff			
Bias (m^3 hr^{-1})	−252	−1.3	−0.8 to 2.6
Correlation	—	0.964	0.86 to 1

Note: The column in the right (Models in IH-MIP2) shows the metrics in terms of observed ranges from all models.

by a more gradual decrease of storage in the following days. JULES-GFB shows similar behaviour with slightly larger amplitude than other models, suggesting a faster decrease in storage from approximately day three. JULES-FD has a very distinctive behaviour, with saturated storage almost completely draining within the first timestep. This fast drying behaviour is consistent with the physical processes highlighted previously in the column experiment for JULES-FD (Figure 5).

Furthermore, the initial increase in unsaturated storage of JULES-GFB is consistent with the initial drop of the water table (Figure 7b). At the end of the first day, the water table has returned to the initial condition and starts to contribute to the outlet streamflow. After the first day, there is increase of unsaturated storage that is linked to the contribution to the runoff for almost all the models. JULES-GFB shows similar behaviour with slightly larger amplitude than the other models, suggesting a faster increase in storage from approximately day three. On the other hand, JULES-FD simulation deviates drastically from the other models resulting in very high bias and low correlation against the benchmark model (Table 2).

Finally, Figure 7c presents the outlet discharge produced by the contribution to the surface runoff, as there is no rainfall in this experiment and no other source of runoff generation rather than the groundwater. At the end of the first day, all the models, except JULES-FD, start to produce surface runoff almost at the same time. The models (except JULES-FD) follow the same behaviour and dynamics with different magnitude. JULES-GFB produces lower values of outlet discharge than any of the IH-MIP2 models. It appears that JULES-GFB produces more unsaturated storage compared with the benchmark (Figure 7a,b and Table 2), possibly indicating that JULES-GFB retains more water in the soil domain compared with the other models, which generate more runoff. Overall, JULES-GFB shows similar magnitude and dynamics compared with other models with metrics of bias and linear correlation to be within the model envelope. JULES-FD does not produce any runoff, as would be expected. Soil water fluxes are exclusively vertical and hence the water leaves the bottom of the soil domain without contributing to runoff generation.

3.3 | Regional experiment

We carry out a comparison between both JULES models by setting up a regional domain experiment in the UK, where groundwater contributes significantly to streamflow. We assess the results in three ways: (1) by analysing spatial patterns of soil moisture, (2) by comparing modelled and simulated domain-average evapotranspiration and (3) by comparing modelled and observed runoff at selected catchments within the domain. For JULES-FD, we tested different values of b exponent (b_{pdm}) from zero (the 'JULES-FD-noPDM' case) to 1 (the 'JULES-FD-PDM' case), following the discussion at Section 2.3.3. The test of multiple b_{pdm} values represents an extra parameter calibration step in JULES-FD which is not needed in JULES-GFB.

3.3.1 | Spatial patterns of soil wetness

We first begin by assessing the behaviour of JULES in reproducing spatial patterns of soil moisture within the regional domain. Figure 8a,b shows the annual average soil wetness for the 5-year period (2008–2012) at the upper soil layer (0–20 cm) for JULES-FD-noPDM and JULES-FD-PDM b_{pdm} = 1, respectively. Both simulations suggest a much smoother spatial pattern without being able to capture similar patterns from the river flow network and topography (Figure 3, top left). The results from both JULES model simulations suggest relatively drier conditions in the northeast region of the domain, which is likely due to this region being characterized by relatively coarser soil (Figure 3, bottom) and also receiving less precipitation when compared with the west region of the domain (i.e., the west region receives annually about 1,200 mm $year^{-1}$ compared with about 700 mm $year^{-1}$ in the east region of the domain; data not shown). This could explain the heterogeneity of Figure 8a,b.

The spatial pattern of soil moisture for JULES-GFB differs drastically from both JULES-FD simulations (Figure 8c), showing a distinct river network of saturated areas as a result of the convergence of groundwater in JULES-GFB. The pattern resembles quite satisfactorily the observed river network (Figure 3, top left). Soil type (coarse vs. fine) continues to play a role in controlling soil moisture dynamics with the north-eastern region of the domain (relatively coarser soils as in Figure 3, bottom), suggesting drier conditions compared with the rest of the domain. We found no strong control by the land cover (Figure 3, top right) on annual soil moisture conditions, which is expected in more humid (cold) regions such as in Wales.

Figure 9 depicts the daily soil wetness fraction, as a domain average for the upper 20 cm for JULES-FD b_{pdm} = 1 against JULES-GFB. We present the JULES-FD b_{pdm} = 1 case because after the calibration of b_{pdm} in JULES-FD against observed runoff, the optimal value for b_{pdm} was equal to 1 for five out of six catchments. Note that the results do not change dramatically for soil wetness, if we use another configuration for PDM. The first observation is that JULES-GFB is much wetter, especially during the summer months (June–August) with soil wetness value about 0.7, when for JULES-FD is less than 0.5. The second observation is about the low values of JULES-FD during the winter months (December–February). For JULES-FD, it is

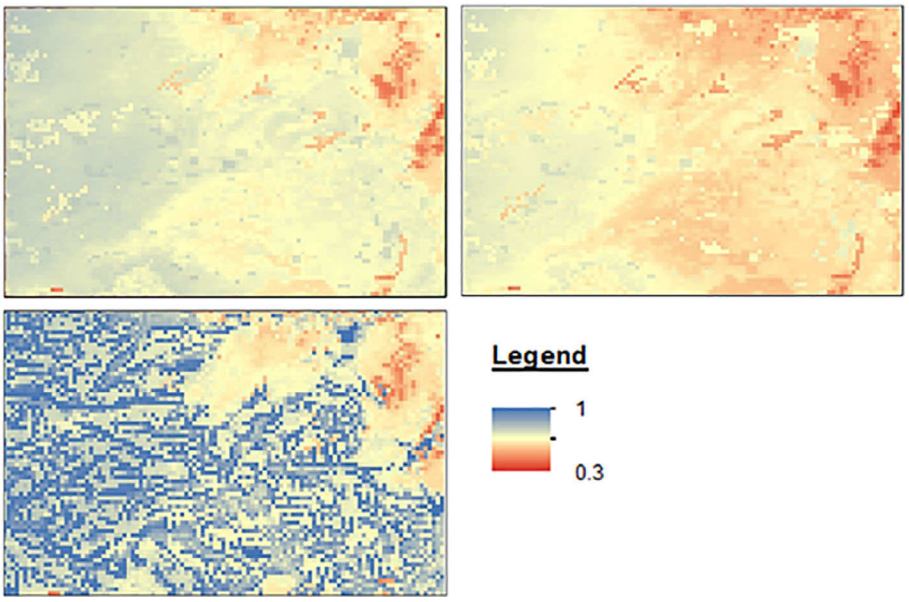

FIGURE 8 Annual average relative saturation of first soil layer (0–20 cm) obtained for the entire 2008–2012 period from (a) JULES-FD-noPDM, (b) JULES-FD-PDM (with b_{pdm} = 1) and (c) JULES-GFB, for the regional domain experiment

unusual to have soil wetness values above 0.7, even for months with high precipitation. Finally, the annual range of soil wetness seasonality is much lower for JULES-FD compared with JULES-GFB.

3.3.2 | Domain-average evapotranspiration

Since this part of the UK is not a water-limited area, the impact of GW model on the simulation of evapotranspiration (ET) is expected to be low, particularly on the annual basis. Nevertheless, we evaluate JULES simulated ET against the GLEAM ET product (Figure 10). Monthly time-series of ET for the study period indicate that more pronounced differences are expected to occur over the summer period with little or no differences observed in the wintertime (Figure 10, left). During summertime, more realistic and relatively wetter soil moisture conditions within the domain (Figure 8) obtained with JULES-GFB, resulting in a slightly increase in ET rates over the summer approaching GLEAM ET's estimates. The overall bias obtained

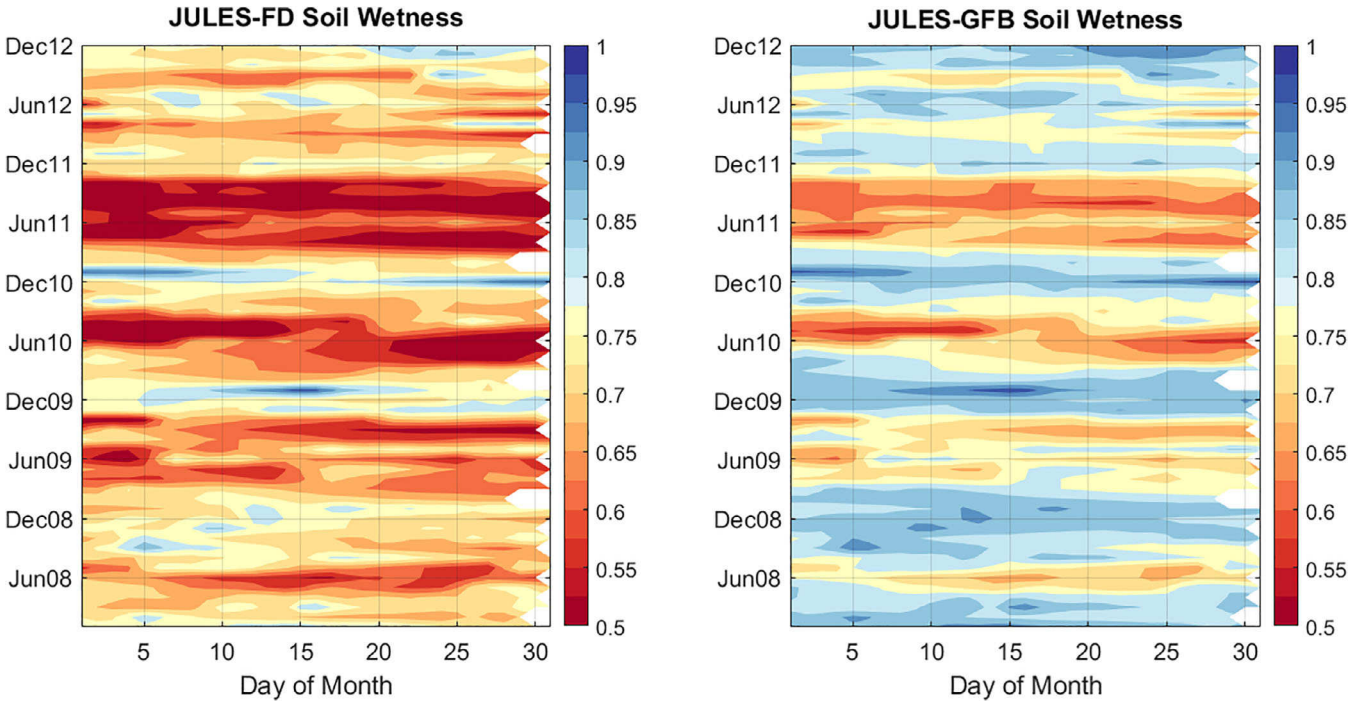

FIGURE 9 Domain-average daily soil moisture for upper 20 cm for JULES-FD b_{pdm} = 1 (left) compared with JULES-GFB (right), for the regional experiment. The figure shows day of the month in the horizontal axis and months increasing from 2008 to 2012 in the vertical axis to better highlight winter and summer seasons

with daily ET estimates computed for JULES-FD relative to GLEAM is −0.22 mm day^{-1}, whereas the mean bias for JULES-GFB relative to GLEAM reduces to −0.01 mm day^{-1}.

In previous sections, we highlighted the strong link between soil type and performance of JULES-GFB given the underlying assumptions of the groundwater parameterizations discussed in Section 2.2 and in more detail by Rahman et al. (2019). In order to further understand this behaviour, we have computed the mean bias for four individual categories of soil types found within the domain (Figure 10, right). In this case, we focus on the summertime period defined to be between April and October. Our results suggest that for all types of soils within the domain, JULES-GFB biases are relatively lower than that those obtained with JULES-FD when compared against GLEAM ET product. Notice that the regional domain does not necessarily show a large range of predominant soil types (Figure 3, bottom). Despite the similarities between the boxplots obtained for JULES-FD and JULES-GFB, we notice that the relative improvement (i.e., bias reduction here taken from the median) in JULES-GFB compared with JULES-FD tend to be larger for the two 'coarser' soil types (silty clay loam and medium sandy loam) and smaller for the two 'finer' soil types (clay loam and clay). As we expect the limitations of free drainage assumptions to be more pronounced in relatively coarse soil types, the performance improvement by adding the groundwater parameterization in those soils is expected to result in more impact than in clay soils, where soil water dynamics are relatively slow and the limitations of assuming free drainage are reduced.

3.3.3 | Total runoff at catchment scale

Figure 11 presents the runoff time-series for one catchment for a subset of the simulation period. The upper subplot compares the performance of JULES-GFB against JULES-FD-noPDM. The performance of JULES-FD-noPDM in reproducing the total runoff is very weak with consistently missing runoff peaks and eventually capturing the large events only, while still showing lower peak magnitudes. The reason is that only the infiltration excess mechanism is activated, so the rainfall rate should be higher than the infiltration rate to produce surface runoff. On the other hand, JULES-GFB tends to capture more accurately the dynamics of the total runoff with some remaining limitations in reproducing low river flows. It seems that the contribution of the baseflow to the total runoff improves the runoff predictions. The bottom panel of Figure 11 depicts the same comparison between JULES-GFB and JULES-FD against observations, but now JULES-FD is run with PDM enabled and with b_{pdm} set to 1 (i.e., assuming an extra calibration step is taken with JULES-FD). Notably, the use of PDM improves remarkably the performance of JULES-FD, suggesting similar behaviour as seen in JULES-GFB. The KGE metric computed relative to the observations was found to increase from 0.22 to 0.51 for the JULES-FD before and after introducing the PDM with the calibrated parameter, respectively; while the KGE obtained for JULES-GFB is 0.74. Notice that in the case of JULES-FD with PDM, a further calibration step is required hence adding an extra level of complexity in the model, which is not needed in JULES-GFB, also limiting JULES applications in places where observations are not necessarily readily available.

The overall performance of the different JULES versions in reproducing total runoff at the selected catchments within the regional domain is summarized in Figure 12 using multiple performance metrics. In this case, the comparison is carried out against observations for three distinct model versions: JULES-FD without PDM, JULES-FD with PDM testing several values for b_{pdm} and JULES-GFB. The decision to show JULES-FD with PDM with multiple b_{pdm} parameters is to

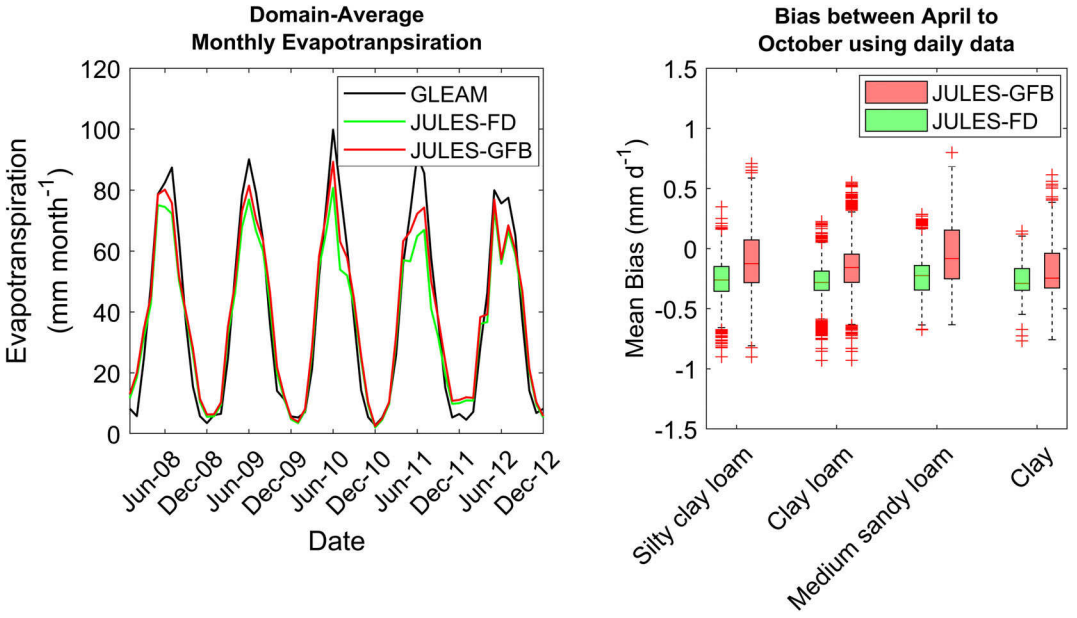

FIGURE 10 Left: Comparison of domain-average monthly evapotranspiration from GLEAM (black), JULES-FD (green) and JULES-GFB (red). Right: Mean bias compute relative to daily evapotranspiration estimates from GLEAM between April and September ('summer' season) and combined into four dominant soil types in the regional domain

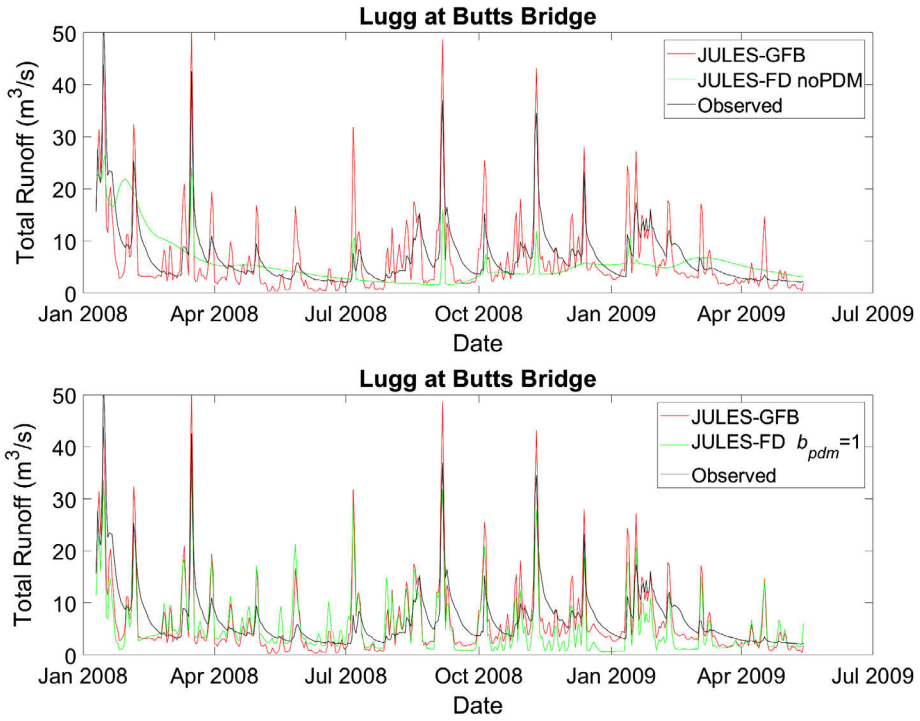

FIGURE 11 Comparison of simulated runoff time-series from JULES-GFB (red) and JULES-FD-noPDM (green) against observed runoff for the Lugg at Butts Bridge catchment for a subset of the simulation period. The difference between top and bottom figure relates to the version of JULES-FD used: JULES-FD-noPDM is shown in the top panel, while JULES-FD with PDM parameter b_{pdm} set to 1

highlight (1) the overall uncertainty range associated with the feasible range of b_{pdm} (e.g., if the model is applied at a data-poor catchment without calibration) and (2) if a calibration step (despite being depicted very simply here) can be achieved (e.g., in catchments where supporting observations can be used for calibration). Our results are focused on three metrics: (1) KGE which aims to show the overall model performance using a typical performance metric adopted in streamflow statistics, (2) linear correlation which will focus on the ability to reproduce the dynamics of the observations and (3) mean bias as an indicator of systematic underestimation or overestimation by the different models. Notice that these metrics are intrinsic relates (Gupta et al., 2009), but there are benefits in studying them separately.

In all catchments investigated within the domain, JULES-GFB performs best (with the exception for two catchments with respect to KGE metrics) (Figure 12). In addition, JULES-FD without PDM (i.e., without any calibration attempt) has the overall worst performance across all six catchments and metrics. KGE values for JULES-FD-no-PDM are low around 0.20–0.30 range (Figure 12a). A possible calibration step taken with JULES-FD using PDM suggests that improvements are achievable and can reach KGE values up to 0.5–0.70 range at different catchments. The KGE values obtained by JULES-GFB have similar low values compared with JULES-FD with PDM (i.e., around 0.5) with the top KGE values around 0.80. Looking in the literature if these KGE values are within the accepted boundaries, we find different limits. Saraiva Okello, Masih, Uhlenbrook, Jewitt, and Van der Zaag (2018) considered values of KGE less 0.5 as *poor*, between 0.5 and 0.7 as *acceptable* and above 0.7 as *good*. Poméon, Diekkrüger, and Kumar (2018) and Rajib, Merwade, and Yu (2016) considered as acceptable models with KGE above 0.5. Gutenson, Tavakoly, Wahl, and Follum (2019) classified KGE as acceptable for KGE between 0 and 0.4, as good for KGE between 0.4 and 0.7 and very good for KGE values above 0.7, following Tavakoly et al. (2017). Considering the above classifications, we could say that JULES-GFB is very good for four out of six catchments and acceptable or good for the other two catchments.

In relation to reproducing the streamflow dynamics from observations, JULES-GFB shows the highest computed linear correlation coefficients at all catchments ranging from 0.60 to 0.80 (Figure 12b). The 'best' JULES-FD with PDM version shows slightly lower coefficients around 0.55–0.75, while the linear correlation coefficients obtained with JULES-FD without PDM are around 0.50. Finally, an important aspect in understanding model performance is to be able to identify any systematic conditions for over- or underpredicting hydrological fluxes such as the runoff. Systematic biases vary from catchment to catchment (Figure 12c); however, JULES-GFB is the only model version which consistently predicts streamflow with lowest biases when compared with JULES-FD without PDM, which appears to highly underestimate river flows (except for one catchment with the lowest BFI). If JULES-FD utilizes the PDM parameterization, biases are reduced across the six catchments but not to the same magnitude as seen with JULES-GFB. In summary, Figure 12 indicates that JULES-GFB is capable of predicting river flows satisfactorily (high KGE) with realistic dynamics (high linear correlation coefficients) and low systematic biases with respect to observations and when compared with the other JULES versions without explicitly representing groundwater processes.

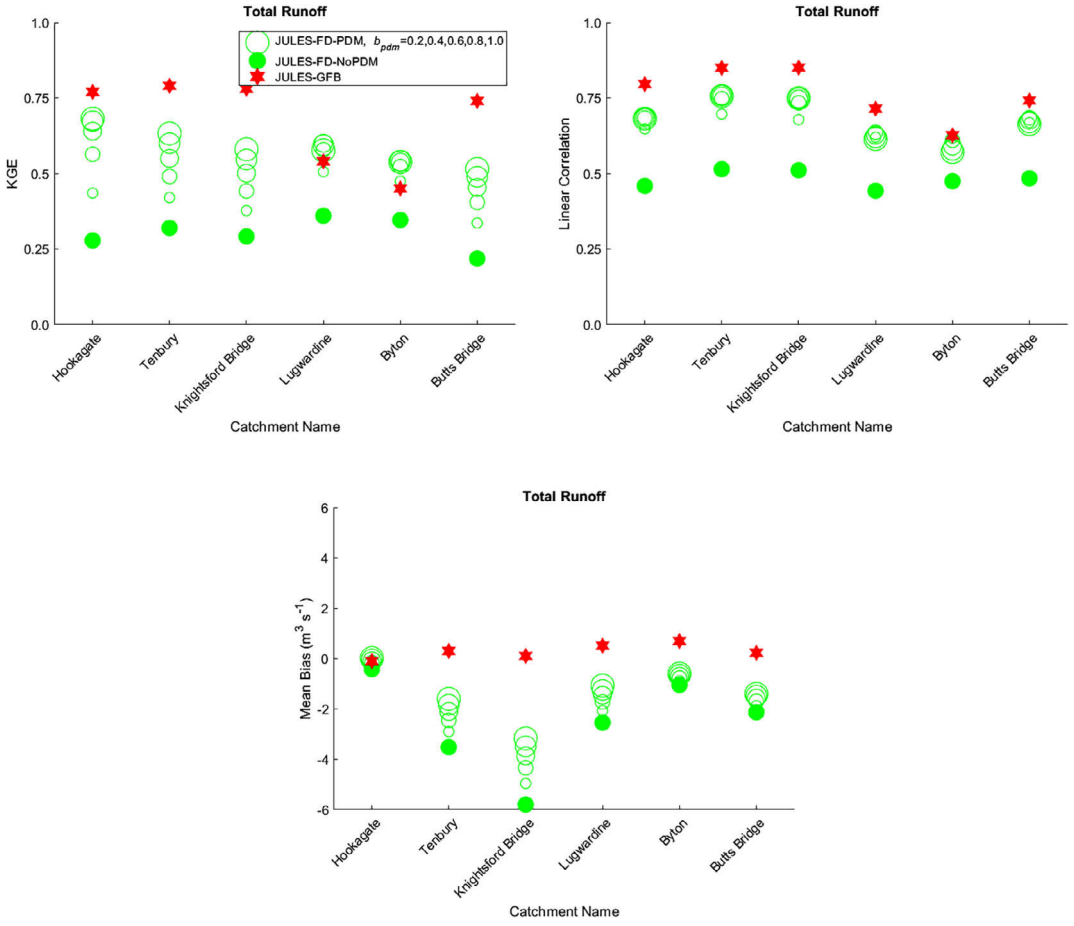

FIGURE 12 Model performance summary across three selected metrics: KGE (top left), linear correlation (top right) and mean bias (bottom) computed from simulated total runoff against observations. The metrics obtained for JULES-FD without PDM are shown as the closed green circles, while the open circles correspond to results obtained from JULES-FD with PDM with varying b_{pdm} (relative to size of the circle); JULES-GFB metrics are shown as red stars

4 | DISCUSSION

We have organized this section in order to answer the two specific research questions highlighted in Section 1. First, we discuss the direct impacts of introducing this new groundwater parameterization in JULES, focusing on understanding the conditions, which result in more or less pronounced improvements in the simulated soil water dynamics (Section 4.1). Then, we discuss the overall impact of such implementation on other hydrological fluxes that are related to soil water dynamics (Section 4.2).

4.1 | Direct impact of new groundwater scheme on simulated soil water dynamics

We examined the behaviour of the JULES model under different conditions using the classic free drainage approach and with our newly proposed groundwater parameterization, respectively. These distinct conditions are tested by altering two physical controlling factors (soil type and position of water table) that are expected to exert some impact on simulated water dynamics in the soil (e.g., Niu et al., 2007; Rahman et al., 2019). From the column scale experiment (Section 3.1), we can highlight two significant findings, which are more directly summarized in Figure 6. First, we found substantial improvements in representing groundwater table dynamics when explicitly incorporating groundwater processes into JULES for all soil types when the water table is initialized closer to the surface and within the soil domain (i.e., from surface to 3 m deep). In this case, fine soil types tend to result in slightly better improvements when compared with the simulations from relatively coarse soils. This behaviour is expected given the nature and assumptions made with the proposed groundwater parameterization. On the other hand, the classic free drainage approach simulates systematic drier conditions for all soil types because it promotes relatively faster dynamics that are solely controlled by the gravity flow downwards without any physical constraint at the bottom of the soil domain. Shallow water regions account for 22–32% of the land globally (Fan et al., 2013); therefore, we expect that the limitations of the free drainage can lead to substantial impact over large regions in global applications when using the default JULES model, those being for hydrological services directly or to account for the interactions between the subsurface–surface–atmosphere.

Our second interesting result relates to the fact that despite promoting substantial improvements in representing soil water dynamics when the water table is initialized at relatively shallow depths, we found little differences between the classic free drainage and the new groundwater scheme for those cases where the initial water table is located relatively deeper and outside of the soil domain (below 3 m). In this case, the complexity of adding a new groundwater scheme into JULES may not be fully justified if the purpose of the model application is to track or depend only on knowing the soil moisture conditions within the soil domain. This is because both JULES-FD and JULES-GFB results agree satisfactorily with the benchmark model used in this study. Studies in the past have suggested groundwater may not exert strong controls to the near-surface soil dynamics when it is far from the surface (Maxwell & Kollet, 2008; Ferguson & Maxwell, 2010; Lo & Famiglietti, 2010). However, the use of JULES-GFB even for deep aquifer systems may be justified if the purpose is to use JULES applied to water resources studies where a representative volume of subsurface water is a key component of the study (de Graaf et al., 2017; Fan et al., 2013).

The purpose of this study is to introduce this new approach by combining a series of synthetic and real-case experiments as recently supported by the hydrological community (e.g., Clark et al., 2015; Kim, Warnock, Ivanov, & Katopodes, 2012; Lee & Chang, 2005; Sulis et al., 2010). It is beyond the scope of this study to test the JULES model using the single-column experiment under several different combinations of factors. The experiments we have selected allowed us to select key factors (soil type and initial water table depth) in order to compare directly against previously published studies (Kollet et al., 2017; Rahman et al., 2019). In doing so, we have limited the number of potential combinations to test, for example, by not investigating the role of rainfall intensity and duration on the model simulations. This was partially mitigated by introducing a real-case experiment in a region with groundwater-dominated catchments in addition to the synthetic cases.

4.2 | Indirect impact of new groundwater scheme on other hydrological fluxes

Implementing the new groundwater parameterization into JULES has led to changes in soil water dynamics, especially when the water table is initialized closer to the surface and within the model soil domain. It is also important to understand how those changes in soil moisture dynamics affect other hydrologically relevant fluxes. Here, we focus on two specific fluxes, namely, the total runoff and evapotranspiration. We first investigated changes in simulated total runoff with a synthetic catchment by comparing our results against the benchmark model, as well as other integrated hydrological models (Figure 7 and Table 2). In summary, we found that JULES-GFB is capable of reproducing the characteristics of multiple storage components and the outlet discharge satisfactorily. Performance metrics from JULES-GFB computed against the benchmark model are well within the range obtained with all other models (Table 2). The exception being only the fact that JULES-GFB had the lowest mean bias for outlet discharge ($-1.3\ m^3\ hr^{-1}$) than the lowest value obtained with the other evaluated models ($-0.8\ m^3\ hr^{-1}$). This suggests that JULES-GFB underestimated the discharge when compared with all other IH-MIP models (Figure 7c), possibly due to relative higher water retention in its soil domain. Nevertheless, the fact that the JULES-GFB model incorporates a mechanism to deal with lateral redistribution of water resulted in the displacement of water and ultimately leading to discharge of the outlet. This mechanism is nonexistent in JULES-FD; hence, only vertical water flow is promoted at individual columns (grid points) in the synthetic catchment, which results in no occurrence of discharged (note: discharge occurs solely by groundwater contribution, as there is no net rainfall forcing imposed at the surface).

In addition to the simulations with the exact specifications from Kollet et al. (2017), we also ran the tilted-V catchment for the 12 different soil types using the same hydraulic properties with the infiltration column-scale experiment. Within the simulation time, only three out of 12 soil types could produce runoff, namely, the sand, the loamy sand and the silt loam. These three soil types have high value of saturated conductivity; thus, they react fast to the groundwater contribution by producing runoff in the outlet. It seems that the higher value of saturated conductivity gives faster and greater peak discharge. It is something we expected, as the timing is linked with the speed of groundwater contribution (saturated conductivity) and the magnitude of discharge is linked with the storage of the aquifer (specific yield). Soil types with lower saturated conductivity values respond much slower to the groundwater table, so they cannot produce runoff within the simulation time (5 days). This proves that sandy soil types are more sensitive to the groundwater parameterization compared with other soil types. Considering the saturated and unsaturated storage curves for different soil types, we find that sand, silt loam and the simulation from the tilted-V experiment (Section 3.2) have linear curves with small fluctuations that show that they change slowly, whereas the silt loam soil type has a more responsive behaviour. It produces runoff only for a few hours, whereas the response of saturated and unsaturated storages shows a dynamic response.

Synthetic experiments have the benefit of allowing nearly full control of the results by comparing model simulations against a benchmark (reference) model taken to be the truth. These experiments allow us to more easily isolate relevant processes for analysis usually representing ideal conditions, which do not necessarily correspond to reality. In order to get a better sense of how our proposed JULES-GFB performs under more realistic conditions, we performed a 5-year simulation over a regional domain in the UK characterized by groundwater-dominated catchments. We investigated the ability of JULES-GFB to accurately represent the spatial patterns of wetness associated with the river network in the region (Figure 8) as well as potential improvements to simulated evapotranspiration (Figure 10) and river discharge (Figure 12) when compared against independent observations.

Our initial analysis within the domain highlights the importance of groundwater process and more specifically the role of lateral flow now being resolved in JULES-GFB in order to allow more realistic

patterns of soil wetness within the domain (Figure 8). These patterns are consistent with two key characteristics of the region, namely, topography and soil type. This is consistent to our initial findings using the synthetic experiments highlighting the various model simulations for different soil types, initial water table depths and with a synthetic catchment whose processes are driven entirely by groundwater dynamics (i.e., no net rainfall forcing). Unlike JULES-GFB, the JULES versions with the classic free drainage are unable to represent such patterns simply because they do not resolve lateral flow and hence all soil water dynamics happen vertically, meaning water eventually leaves the soil domain from the model without allowing for the low elevation areas to properly show convergent patterns. The more realistic water dynamics and ability to retain the water within the soil domain due to a newly imposed bottom boundary condition in the soil domain was also reported by (Niu et al., 2007).

The analysis from Figure 8 allows us to have some confidence in the model performance. However, they do not directly quantify potential improvement in model performance. Therefore, we further investigate whether this arguably more realistic behaviour of the model results in improved evapotranspiration (ET) fluxes. As expected in this humid but energy limited region, the impacts of introducing the new JULES-GFB scheme indicates more pronounced changes during the summer season ET (Figure 10) with slightly increase in simulated ET compared with JULES-FD, resulting in slightly more consistent estimates when compared with the GLEAM ET product. Our overall results also indicate that simulated ET from JULES-GFB shows reduced biases compared with JULES-FD, which tends to underestimate ET fluxes. This behaviour is consistent across the main soil types observed in the regional domain. Similar results were also previously suggested by a number of studies (Huang et al., 2019; Nie et al., 2018; Niu et al., 2007; Yeh and Eltahir, 2005a; York et al., 2002) by comparing against observations from the water balance equation, ground based measurements and remote sensing products.

Finally, we look at the results summarizing JULES-GFB's ability to reproduce river discharge in comparison with discharge observations at six catchments within the domain (all strongly dominated by groundwater processes, given their relatively high Base Flow Indices—BFI). We highlight the performance of the model by (1) employing a metric typically used for evaluating model performance of streamflow predictions (KGE), (2) analysing the ability of the model to reproduce similar dynamics from the observed record (linear correlation coefficient) and (3) identifying any unwanted systematic biases in the model (mean bias). Particularly for JULES-FD, we also tested an additional calibration step (which is not applied to JULES-GFB) by enabling the PDM scheme in the model that empirically tries to resolve any limitations related to soil saturation distribution at subgrid spatial scales. In summary, our results suggest that JULES-GFB performance is superior for nearly all metrics and catchments (Figure 12). The majority of KGE values obtained are above 0.75, which suggest satisfactory performance, whereas JULES-FD without PDM shows KGE values on the order of 0.25. Similar conclusions about the performance of JULES-GFB in comparison with JULES-FD without PDM can be drawn for the linear correlation coefficient and the mean bias. Previous studies reported improvements on the same order of magnitude (Maxwell & Miller, 2005; Yeh and Eltahir, 2005a; Vergnes & Decharme, 2012; York et al., 2002). Interestingly, if JULES-FD is applied with a calibrated version of PDM, its performance improves substantially, but still does not exceed the performance of our JULES-GFB. We argue, however, that any additional calibration step introduced in this case will likely require a priori estimation of the parameters associated with PDM. This will likely require the availability of independent observations used for the calibration period, hence undermining the performance of JULES-FD particularly for hydrological applications in data-poor regions and eventually continental to global applications. It is important to stress that despite the observed improvements with JULES-FD with PDM, this version of the model still lacks the explicitly representation of groundwater processes.

Note that our approach is different from other previous studies. For instance, the developed approach by Niu et al. (2007) and Huang et al. (2019) extracts the baseflow from the aquifer, as a percentage of the storage or the water table depth using an exponential function. In our study, the flux of baseflow comes from the contribution of aquifer to the soil domain by an additional upward flux component. Other models employ an uncoupled representation of groundwater (e.g., de Graaf et al., 2015, 2017; Fan & Miguez-Macho, 2011). According to this approach, the output of the GW model feeds the bottom boundary condition of the LSM. Both models run separately, and, in this way, there is not a real-time feedback between saturated and unsaturated zones, whereas the GW model is not dynamically updated. In our case, we implement a dynamic model that can give us a more accurate insight for the surface subsurface interactions. Furthermore, our model adopts a simplified approach to represent groundwater in two dimensions. Three-dimensional groundwater coupling, such as Maxwell et al. (2011) and Tian et al. (2012), requires substantial computational resources, especially for large-scale applications. Our approach is extensively evaluated against similarly more complex 3-D hydrological models to ensure much of its realism is maintained during the development phase, while identifying potential limitations and shortcomings.

This approach and this methodology have some limitations. First, we tested the model over some regional domain characterized by groundwater dominated catchments. We recognize that the region is still relatively small compared with potential applications of the model at continental or global scale. Furthermore, the selected regional domain has climatic conditions that known to have weak interactions with the atmosphere (i.e., weak soil moisture-ET interactions). Regarding the characteristics of the new approach, our simplified 2-D approach has limitations compared with the more realistic 3-D approach. In order to examine the magnitude of this limitation, both the theoretical development study (Rahman et al., 2019) and this study employed synthetic experiments to evaluate how much this approach impacts the overall realism of the simulation by benchmarking our simulations with a 3-D hydrological model ParFlow. We did not find significant differences between the 2-D (JULES-GFB) and the 3-D (ParFlow) approach that proves the realism of our

approach. Finally, despite these limitations, our study suggests substantial improvement in the JULES model, which is a typical LSM that currently does not represent soil–aquifer interactions in its operational version.

5 | CONCLUSIONS

In this study, we incorporate a simplified groundwater representation in the Joint UK Land Environment Simulator (JULES) and investigate the impacts of this implementation on land surface hydrological processes. We consider two synthetic (a single-column and a tilted-V) and one real-world (regional domain including six catchments in the UK) test cases to demonstrate the impacts of representing groundwater explicitly in JULES-GFB. The performance of JULES-GFB is evaluated by considering a 3-D groundwater flow model ParFlow as the benchmark for the synthetic test cases. For the real-world test case, observed runoff and evapotranspiration data are used for the model evaluation.

Results from the synthetic test cases demonstrate that JULES-GFB improves soil moisture dynamics and runoff generation process compared with the default JULES-FD, especially for fine-textured soils. The real-world test case demonstrates that JULES-GFB improves the prediction of runoff and evapotranspiration compared with JULES-FD. From this test case, it can also be concluded that representing groundwater hydrology explicitly can supersede the advantage of implementing a calibrated saturation excess runoff generation scheme in JULES.

JULES-GFB shows some limitations in reproducing soil moisture dynamics and runoff generation compared with the benchmark model for coarse-textured soils. This is expected because of the simplifying assumptions considered for coupling the groundwater parametrization with JULES. These assumptions are necessary to achieve a high computational efficiency of the model (Rahman et al., 2019). In this regard, our proposed approach of representing groundwater hydrology aligns with the objectives of the recent development efforts of hydro-JULES (Dadson et al., 2019) and other land surface and hydrological models for large-scale applications (Clark et al., 2015; Gleeson et al., 2019).

The real-world test case presented here is limited in term of hydrogeological and climatic conditions because this is the first study that evaluates the newly developed JULES-GFB model. This model requires further testing under different hydrogeological and climatic conditions, which should be the subject of further research. Subsequently, JULES-GFB could potentially be used as a numerical tool to assess water resources under, for example, future climate change and land use/cover change scenarios.

DATA AVAILABILITY STATEMENT

The data that support the findings of this study are openly available at https://eip.ceh.ac.uk/chess, https://nrfa.ceh.ac.uk/data/search and after request here https://www.gleam.eu/

ACKNOWLEDGEMENTS

This work was funded by the Engineering and Physical Sciences Research Council (EPSRC) Water Informatics: Science and Engineering Centre for Doctoral Training (WISE-CDT) (grant number EP/L016214/1). Additional support from the A MUlti-scale Soil moisture-Evapotranspiration Dynamics study (AMUSED) (grant number NE/M003086/1) and the Brazilian Experimental datasets for MUlti-Scale interactions in the critical zone under Extreme Drought (BEMUSED) (grant number NE/R004897/1) projects both funded by Natural Environment Research Council (NERC). The soils dataset was provided by the Cranfield University (National Soils Resource Institute) and for the Controller of HMSO 2019 under the licence agreement L0155/00977. We would also like to thank the associate editor and two anonymous reviewers who provided valuable feedback and suggestions to improve the article.

ORCID

Stamatis-Christos Batelis https://orcid.org/0000-0002-9770-4738

REFERENCES

Abbott, M. B., Bathurst, J. C., Cunge, J. A., O'connell, P. E., & Rasmussen, J. (1986). An introduction to the European hydrological system—Systeme Hydrologique Europeen,"SHE", 2: Structure of a physically-based, distributed modelling system. *Journal of Hydrology*, *87*(1–2), 61–77.

Alley, W. M., Healy, R. W., LaBaugh, J. W., & Reilly, T. E. (2002). Flow and storage in groundwater systems. *Science*, *296*(5575), 1985–1990.

Aquanty, I. (2015). *HydroGeoSphere user manual* (p. 435). Waterloo: Ont.

Ashby, S. F., & Falgout, R. D. (1996). A parallel multigrid preconditioned conjugate gradient algorithm for groundwater flow simulations. *Nuclear Science and Engineering*, *124*(1), 145–159.

Bakopoulou, C., 2015. Critical assessment of structure and parameterization of JULES land surface model at different spatial scales in a UK Chalk catchment.

Beck, H. E., van Dijk, A. I., de Roo, A., Dutra, E., Fink, G., Orth, R., & Schellekens, J. (2017). Global evaluation of runoff from ten state-of-the-art hydrological models. *Hydrology and Earth System Sciences*, *21*(6), 2881–2903.

Bell, V. A., Kay, A. L., Jones, R. G., & Moore, R. J. (2007). Development of a high resolution grid-based river flow model for use with regional climate model output. *Hydrology and Earth System Sciences Discussions*, *11*(1), 532–549.

Best, M. J., Pryor, M., Clark, D. B., Rooney, G. G., Essery, R., Ménard, C. B., … Mercado, L. M. (2011). The Joint UK Land Environment Simulator (JULES), model description—Part 1: Energy and water fluxes. *Geoscientific Model Development*, *4*(3), 677–699.

Bierkens, M. F., Bell, V. A., Burek, P., Chaney, N., Condon, L. E., David, C. H., … Flörke, M. (2015). Hyper-resolution global hydrological modelling: What is next? "Everywhere and locally relevant". *Hydrological Processes*, *29*(2), 310–320.

Bixio, A., Gambolati, G., Paniconi, C., Putti, M., Shestopalov, V., Bublias, V., … Rudenko, Y. (2002). Modeling groundwater-surface water interactions including effects of morphogenetic depressions in the Chernobyl exclusion zone. *Environmental Geology*, *42*(2–3), 162–177.

Butts, M. B., Payne, J. T., Kristensen, M., & Madsen, H. (2004). An evaluation of the impact of model structure on hydrological modelling uncertainty for streamflow simulation. *Journal of Hydrology*, *298*(1–4), 242–266.

Camporese, M., Paniconi, C., Putti, M., & Orlandini, S. (2010). Surface-subsurface flow modeling with path-based runoff routing, boundary condition-based coupling, and assimilation of multisource observation data. *Water Resources Research*, *46*(2), 1–22.

Clark, D. B., & Gedney, N. (2008). Representing the effects of subgrid variability of soil moisture on runoff generation in a land surface model. *Journal of Geophysical Research: Atmospheres*, *113*(D10), 1–13.

Clark, D. B., Mercado, L. M., Sitch, S., Jones, C. D., Gedney, N., Best, M. J., … Boucher, O. (2011). The Joint UK Land Environment Simulator (JULES), model description—Part 2: Carbon fluxes and vegetation dynamics. *Geoscientific Model Development*, *4*(3), 701–722.

Clark, M. P., Fan, Y., Lawrence, D. M., Adam, J. C., Bolster, D., Gochis, D. J., … Maxwell, R. M. (2015). Improving the representation of hydrologic processes in Earth System Models. *Water Resources Research*, *51*(8), 5929–5956.

Condon, L. E., & Maxwell, R. M. (2015). Evaluating the relationship between topography and groundwater using outputs from a continental-scale integrated hydrology model. *Water Resources Research*, *51*(8), 6602–6621.

Coon, E. T., Moulton, J. D., & Painter, S. L. (2016). Managing complexity in simulations of land surface and near-surface processes. *Environmental Modelling & Software*, *78*, 134–149.

Dadson, S., Blyth, E., Clark, D., Hughes, A., Hannaford, J., Lawrence, B., … Reynard, N. (2019, January). Hydro-JULES: Next generation land-surface and hydrological predictions. *Geophysical Research Abstracts*, *21*.

Dadson, S.J. and Bell, V.A., 2010. Comparison of Grid-2-Grid and TRIP runoff routing schemes.

Dadson, S. J., Bell, V. A., & Jones, R. G. (2011). Evaluation of a grid-based river flow model configured for use in a regional climate model. *Journal of Hydrology*, *411*(3), 238–250.

de Goncalves, L.G.G., Restrepo-Coupe, N., da Rocha, H., Saleska, S., & Stockli, R. (2008). The large scale biosphere-atmosphere experiment in amazônia, model intercomparison project (LBA-MIP) protocol. LBA-MIP website: http://www.climatemodeling.org/lba-mip/March,19.

de Graaf, I. D., Sutanudjaja, E. H., Van Beek, L. P. H., & Bierkens, M. F. P. (2015). A high-resolution global-scale groundwater model. *Hydrology and Earth System Sciences*, *19*(2), 823–837.

de Graaf, I. E., van Beek, R. L., Gleeson, T., Moosdorf, N., Schmitz, O., Sutanudjaja, E. H., & Bierkens, M. F. (2017). A global-scale two-layer transient groundwater model: Development and application to groundwater depletion. *Advances in Water Resources*, *102*, 53–67.

Endrizzi, S., Gruber, S., Dall'Amico, M., & Rigon, R. (2014). GEOtop 2.0: Simulating the combined energy and water balance at and below the land surface accounting for soil freezing, snow cover and terrain effects. *Geoscientific Model Development*, *7*(6), 2831–2857.

Famiglietti, J. S., Lo, M., Ho, S. L., Bethune, J., Anderson, K. J., Syed, T. H., … Rodell, M. (2011). Satellites measure recent rates of groundwater depletion in California's Central Valley. *Geophysical Research Letters*, *38*(3), 1–4.

Fan, Y., Li, H., & Miguez-Macho, G. (2013). Global patterns of groundwater table depth. *Science*, *339*(6122), 940–943.

Fan, Y., & Miguez-Macho, G. (2011). A simple hydrologic framework for simulating wetlands in climate and earth system models. *Climate Dynamics*, *37*(1–2), 253–278.

Ferguson, I. M., & Maxwell, R. M. (2010). Role of groundwater in watershed response and land surface feedbacks under climate change. *Water Resources Research*, *46*(10), 1–15.

Forzieri, G., Alkama, R., Miralles, D. G., & Cescatti, A. (2017). Satellites reveal contrasting responses of regional climate to the widespread greening of Earth. *Science*, *356*(6343), 1180–1184.

Ganji, A., & Sushama, L. (2018). Improved representation of surface-groundwater interaction in the Canadian land surface scheme. *International Journal of Climatology.*, *38*, 5077–5094.

Gedney, N., & Cox, P. M. (2003). The sensitivity of global climate model simulations to the representation of soil moisture heterogeneity. *Journal of Hydrometeorology*, *4*(6), 1265–1275.

Givati, A., Gochis, D., Rummler, T., & Kunstmann, H. (2016). Comparing one-way and two-way coupled hydrometeorological forecasting systems for flood forecasting in the Mediterranean region. *Hydrology*, *3*(2), 19.

Gleeson, T., Wagener, T., Doell, P., Bierkens, M., Wada, Y., Lo, M.H., Taylor, R., Rahman, S., Rosolem, R., Hill, M. and West, C., 2019. Groundwater representation in continental to global hydrologic models: a call for open and holistic evaluation, conceptualization and classification.

Gudmundsson, L., Tallaksen, L. M., Stahl, K., Clark, D. B., Dumont, E., Hagemann, S., … Voss, F. (2012a). Comparing large-scale hydrological model simulations to observed runoff percentiles in Europe. *Journal of Hydrometeorology*, *13*(2), 604–620.

Gudmundsson, L., Wagener, T., Tallaksen, L. M., & Engeland, K. (2012b). Evaluation of nine large-scale hydrological models with respect to the seasonal runoff climatology in Europe. *Water Resources Research*, *48*(11).

Gulden, L. E., Rosero, E., Yang, Z. L., Rodell, M., Jackson, C. S., Niu, G. Y., … Famiglietti, J. (2007). Improving land-surface model hydrology: Is an explicit aquifer model better than a deeper soil profile? *Geophysical Research Letters*, *34*(9), 1–5.

Guppy, L., Uyttendaele, P., Villholth, K.G. and Smakhtin, V., 2018. Groundwater and sustainable development goals: Analysis of interlinkages.

Gupta, H. V., Kling, H., Yilmaz, K. K., & Martinez, G. F. (2009). Decomposition of the mean squared error and NSE performance criteria: Implications for improving hydrological modelling. *Journal of Hydrology*, *377*(1–2), 80–91.

Gutenson, J. L., Tavakoly, A. A., Wahl, M. D., & Follum, M. L. (2019). Comparison of generalized non-data-driven reservoir routing models for global-scale hydrologic modeling. *Hydrology and Earth System Sciences Discussions*, 1–41.

Gutowski, W. J., Jr., Vörösmarty, C. J., Person, M., Ötles, Z., Fekete, B., & York, J. (2002). A coupled land-atmosphere simulation program (CLASP): Calibration and validation. *Journal of Geophysical Research: Atmospheres*, *107*(D16), ACL-3.

Guzman, J. A., Moriasi, D. N., Gowda, P. H., Steiner, J. L., Starks, P. J., Arnold, J. G., & Srinivasan, R. (2015). A model integration framework for linking SWAT and MODFLOW. *Environmental Modelling & Software*, *73*, 103–116.

Hallett, S. H., Sakrabani, R., Keay, C. A., & Hannam, J. A. (2017). Developments in land information systems: Examples demonstrating land resource management capabilities and options. *Soil Use and Management*, *33*(4), 514–529.

Houldcroft, C. J., Grey, W. M., Barnsley, M., Taylor, C. M., Los, S. O., & North, P. R. (2009). New vegetation albedo parameters and global fields of soil background albedo derived from MODIS for use in a climate model. *Journal of Hydrometeorology*, *10*(1), 183–198.

Huang, Z., Tang, Q., Lo, M. H., Liu, X., Lu, H., Zhang, X., & Leng, G. (2019). The influence of groundwater representation on hydrological simulation and its assessment using satellite-based water storage variation. *Hydrological Processes*, *33*(8), 1218–1230.

Jackson, C.R., 2001. The development and validation of the object-oriented quasi three-dimensional regional groundwater model ZOOMQ3D.

Johannes Dolman, A., & Gregory, D. (1992). The parametrization of rainfall interception in GCMs. *Quarterly Journal of the Royal Meteorological Society*, *118*(505), 455–467.

Keune, J., Gasper, F., Goergen, K., Hense, A., Shrestha, P., Sulis, M., & Kollet, S. (2016). Studying the influence of groundwater representations on land surface-atmosphere feedbacks during the European heat wave in 2003. *Journal of Geophysical Research: Atmospheres*, *121*(22), 13,301–13,325.

Kim, J., Warnock, A., Ivanov, V. Y., & Katopodes, N. D. (2012). Coupled modeling of hydrologic and hydrodynamic processes including overland and channel flow. *Advances in Water Resources*, *37*, 104–126.

Koirala, S., Kim, H., Hirabayashi, Y., Kanae, S., & Oki, T. (2019). Sensitivity of global hydrological simulations to groundwater capillary flux parameterizations. *Water Resources Research*, *55*(1), 402–425.

Kollet, S., Sulis, M., Maxwell, R. M., Paniconi, C., Putti, M., Bertoldi, G., … Mouche, E. (2017). The integrated hydrologic model intercomparison project, IH-MIP2: A second set of benchmark results to diagnose integrated hydrology and feedbacks. *Water Resources Research*, *53*(1), 867–890.

Kollet, S. J., & Maxwell, R. M. (2006). Integrated surface–groundwater flow modeling: A free-surface overland flow boundary condition in a parallel groundwater flow model. *Advances in Water Resources*, *29*(7), 945–958.

Kollet, S. J., & Maxwell, R. M. (2008). Capturing the influence of groundwater dynamics on land surface processes using an integrated, distributed watershed model. *Water Resources Research*, *44*(2), 1–18.

Le Vine, N., Butler, A., McIntyre, N., & Jackson, C. (2016). Diagnosing hydrological limitations of a land surface model: Application of JULES to a deep-groundwater chalk basin. *Hydrology and Earth System Sciences*, *20*(1), 143–159.

Lee, K. T., & Chang, C. H. (2005). Incorporating subsurface-flow mechanism into geomorphology-based IUH modeling. *Journal of Hydrology*, *311*(1), 91–105.

Lehner, B., Döll, P., Alcamo, J., Henrichs, T., & Kaspar, F. (2006). Estimating the impact of global change on flood and drought risks in Europe: A continental, integrated analysis. *Climatic Change*, *75*(3), 273–299.

Lehner, B., Verdin, K., & Jarvis, A. (2008). New global hydrography derived from spaceborne elevation data. *Eos, Transactions American Geophysical Union*, *89*(10), 93–94.

Lo, M. H., & Famiglietti, J. S. (2010). Effect of water table dynamics on land surface hydrologic memory. *Journal of Geophysical Research: Atmospheres*, *115*(D22), 1–12.

MacKellar, N. C., Dadson, S. J., New, M., & Wolski, P. (2013). Evaluation of the JULES land surface model in simulating catchment hydrology in Southern Africa. *Hydrology and Earth System Sciences Discussions*, *10*(8), 11093–11128.

Martens, B., Waegeman, W., Dorigo, W. A., Verhoest, N. E., & Miralles, D. G. (2018). Terrestrial evaporation response to modes of climate variability. *NPJ Climate and Atmospheric Science*, *1*(1), 43.

Martínez-de la Torre, A., Blyth, E. M., & Weedon, G. P. (2019). Using observed river flow data to improve the hydrological functioning of the JULES land surface model (vn4. 3) used for regional coupled modelling in Great Britain (UKC2). *Geoscientific Model Development*, *12*(2), 765–784.

Maxwell, R. M. (2013). A terrain-following grid transform and preconditioner for parallel, large-scale, integrated hydrologic modeling. *Advances in Water Resources*, *53*, 109–117.

Maxwell, R. M., & Kollet, S. J. (2008). Interdependence of groundwater dynamics and land-energy feedbacks under climate change. *Nature Geoscience*, *1*(10), 665–669.

Maxwell, R.M., Kollet, S.J., Smith, S.G., Woodward, C.S., Falgout, R.D., Ferguson, I.M., Baldwin, C., Bosl, W.J., Hornung, R. and Ashby, S., 2009. ParFlow user's manual. International Ground Water Modeling Center Report GWMI, 1(2009), 129p.

Maxwell, R. M., Lundquist, J. K., Mirocha, J. D., Smith, S. G., Woodward, C. S., & Tompson, A. F. (2011). Development of a coupled groundwater–atmosphere model. *Monthly Weather Review*, *139*(1), 96–116.

Maxwell, R. M., & Miller, N. L. (2005). Development of a coupled land surface and groundwater model. *Journal of Hydrometeorology*, *6*(3), 233–247.

Meenal, M., & Eldho, T. I. (2011). Simulation of groundwater flow in unconfined aquifer using meshfree point collocation method. *Engineering Analysis with Boundary Elements*, *35*(4), 700–707.

Miralles, D. G., Holmes, T. R. H., De Jeu, R. A. M., Gash, J. H. C., Meesters, A. G. C. A., & Dolman, A. J. (2011). Global land-surface evaporation estimated from satellite-based observations.

Moore, R. J. (1985). The probability-distributed principle and runoff production at point and basin scales. *Hydrological Sciences Journal*, *30*(2), 273–297.

Moore, R. J. (2007). The PDM rainfall-runoff model. *Hydrology and Earth System Sciences Discussions*, *11*(1), 483–499.

Morton, D., Rowland, C., Wood, C., Meek, L., Marston, C., Smith, G., Wadsworth, R. and Simpson, I., 2011. Final report for LCM2007—The new UK land cover map. Countryside Survey Technical Report No 11/07.

Nie, W., Zaitchik, B. F., Rodell, M., Kumar, S. V., Anderson, M. C., & Hain, C. (2018). Groundwater withdrawals under drought: Reconciling GRACE and land surface models in the United States high plains aquifer. *Water Resources Research*, *54*(8), 5282–5299.

Niu, G. Y., Yang, Z. L., Dickinson, R. E., Gulden, L. E., & Su, H. (2007). Development of a simple groundwater model for use in climate models and evaluation with gravity recovery and climate experiment data. *Journal of Geophysical Research: Atmospheres*, *112*(D7), 1–14.

Painter, S. L., Coon, E. T., Atchley, A. L., Berndt, M., Garimella, R., Moulton, J. D., … Wilson, C. J. (2016). Integrated surface/subsurface permafrost thermal hydrology: Model formulation and proof-of-concept simulations. *Water Resources Research*, *52*(8), 6062–6077.

Paniconi, C., Aldama, A. A., & Wood, E. F. (1991). Numerical evaluation of iterative and noniterative methods for the solution of the nonlinear Richards equation. *Water Resources Research*, *27*(6), 1147–1163.

Pinder, G. F., & Bredehoeft, J. D. (1968). Application of the digital computer for aquifer evaluation. *Water Resources Research*, *4*(5), 1069–1093.

Poméon, T., Diekkrüger, B., & Kumar, R. (2018). Computationally efficient multivariate calibration and validation of a grid-based hydrologic model in sparsely gauged West African River basins. *Water*, *10*(10), 1418.

Prickett, T.A. and Lonnquist, C.G., 1971. Selected digital computer techniques for groundwater resource evaluation. Bulletin (Illinois State Water Survey), No. 55.

Rahman, M., Rosolem, R., Kollet, S. J., & Wagener, T. (2019). Towards a computationally efficient free-surface groundwater flow boundary condition for large-scale hydrological modelling. *Advances in Water Resources*, *123*, 225–233.

Rajib, M. A., Merwade, V., & Yu, Z. (2016). Multi-objective calibration of a hydrologic model using spatially distributed remotely sensed/in-situ soil moisture. *Journal of Hydrology*, *536*, 192–207.

Reinecke, R., Foglia, L., Mehl, S., Herman, J. D., Wachholz, A., Trautmann, T., & Döll, P. (2019). Spatially distributed sensitivity of simulated global groundwater heads and flows to hydraulic conductivity, groundwater recharge, and surface water body parameterization. *Hydrology & Earth System Sciences*, *23*(11), 4561–4582.

Rigon, R., Bertoldi, G., & Over, T. M. (2006). GEOtop: A distributed hydrological model with coupled water and energy budgets. *Journal of Hydrometeorology*, *7*(3), 371–388.

Robinson, E. L., Blyth, E. M., Clark, D. B., Finch, J., & Rudd, A. C. (2016). Trends in evaporative demand in Great Britain using high-resolution meteorological data. *Hydrology and Earth System Sciences*, *2016*, 1–1.

Saraiva Okello, A. M., Masih, I., Uhlenbrook, S., Jewitt, G. P., & Van der Zaag, P. (2018). Improved process representation in the simulation of the hydrology of a meso-scale semi-arid catchment. *Water*, *10*(11), 1549.

Schaap, M. G., Leij, F. J., & Van Genuchten, M. T. (2001). Rosetta: A computer program for estimating soil hydraulic parameters with hierarchical pedotransfer functions. *Journal of Hydrology*, *251*(3–4), 163–176.

Siebert, S., Burke, J., Faures, J. M., Frenken, K., Hoogeveen, J., Döll, P., & Portmann, F. T. (2010). Groundwater use for irrigation—A global inventory. *Hydrology and Earth System Sciences*, *14*(10), 1863–1880.

Sulis, M., Meyerhoff, S. B., Paniconi, C., Maxwell, R. M., Putti, M., & Kollet, S. J. (2010). A comparison of two physics-based numerical models for simulating surface water–groundwater interactions. *Advances in Water Resources*, *33*(4), 456–467.

Sutanudjaja, E. H., Van Beek, R., Wanders, N., Wada, Y., Bosmans, J. H., Drost, N., … Karssenberg, D. (2018). PCR-GLOBWB 2: A 5 arcmin global hydrological and water resources model. *Geoscientific Model Development*, *11*(6), 2429–2453.

Tan, T. S., Phoon, K. K., & Chong, P. C. (2004). Numerical study of finite element method based solutions for propagation of wetting fronts in unsaturated soil. *Journal of Geotechnical and Geoenvironmental Engineering*, *130*(3), 254–263.

Tavakoly, A. A., Snow, A. D., David, C. H., Follum, M. L., Maidment, D. R., & Yang, Z. L. (2017). Continental-scale river flow modeling of the Mississippi River basin using high-resolution NHDPlus dataset. *JAWRA: Journal of the American Water Resources Association*, *53*(2), 258–279.

Tian, J., Liu, J., Wang, Y., Wang, W., Li, C., & Hu, C. (2020). A coupled atmospheric-hydrologic modeling system with variable grid sizes for rainfall-runoff simulation in semi-humid and semi-arid watersheds: How does the coupling scale affects the results? *Hydrology and Earth System Sciences Discussions*, 1–36.

Tian, W., Li, X., Wang, X. S., & Hu, B. X. (2012). Coupling a groundwater model with a land surface model to improve water and energy cycle simulation. *Hydrology and Earth System Sciences Discussions*, *9*(1), 1163–1205.

Van Genuchten, M. T. (1980). A closed-form equation for predicting the hydraulic conductivity of unsaturated soils. *Soil Science Society of America Journal*, *44*(5), 892–898.

Vergnes, J. P., & Decharme, B. (2012). A simple groundwater scheme in the TRIP river routing model: Global off-line evaluation against GRACE terrestrial water storage estimates and observed river discharges. *Hydrology and Earth System Sciences*, *16*(10), 3889.

Weedon, G. P., Prudhomme, C., Crooks, S., Ellis, R. J., Folwell, S. S., & Best, M. J. (2015). Evaluating the performance of hydrological models via cross-spectral analysis: Case study of the Thames Basin, United Kingdom. *Journal of Hydrometeorology*, *16*(1), 214–231.

Weill, S., Mouche, E., & Patin, J. (2009). A generalized Richards equation for surface/subsurface flow modelling. *Journal of Hydrology*, *366*(1–4), 9–20.

Yeh, P. J., & Eltahir, E. A. (2005a). Representation of water table dynamics in a land surface scheme. Part I: Model development. *Journal of Climate*, *18*(12), 1861–1880.

Yeh, P. J., & Eltahir, E. A. (2005b). Representation of water table dynamics in a land surface scheme. Part II: Subgrid variability. *Journal of Climate*, *18*(12), 1881–1901.

York, J. P., Person, M., Gutowski, W. J., & Winter, T. C. (2002). Putting aquifers into atmospheric simulation models: An example from the Mill Creek Watershed, northeastern Kansas. *Advances in Water Resources*, *25*(2), 221–238.

Zeng, Y., Xie, Z., Liu, S., Xie, J., Jia, B., Qin, P., & Gao, J. (2018). Global land surface modeling including lateral groundwater flow. *Journal of Advances in Modeling Earth Systems*, *10*(8), 1882–1900.

Zulkafli, Z., Buytaert, W., Onof, C., Lavado, W., & Guyot, J. L. (2013). A critical assessment of the JULES land surface model hydrology for humid tropical environments. *Hydrology and Earth System Sciences*, *17*(3), 1113–1132.

SUPPORTING INFORMATION

Additional supporting information may be found online in the Supporting Information section at the end of this article.

How to cite this article: Batelis S-C, Rahman M, Kollet S, Woods R, Rosolem R. Towards the representation of groundwater in the Joint UK Land Environment Simulator. *Hydrological Processes*. 2020;34:2843–2863. https://doi.org/10.1002/hyp.13767